Journal of Geochemical Exploration 159 (2015) 148–168

Contents lists available at ScienceDirect

Journal of Geochemical Exploration

journal homepage: www.elsevier.com/locate/jgeoexp

Distribution, mineralogy and geochemistry of silica-iron exhalites and related rocks from the Tyrone Igneous Complex: Implications for VMS mineralization in Northern Ireland

Steven P. Hollis [a,b,*], Mark R. Cooper [c], Richard J. Herrington [d], Stephen Roberts [a], Garth Earls [e], Alicia Verbeeten [f], Stephen J. Piercey [g], Sandy M. Archibald [h]

[a] Ocean and Earth Science, National Oceanography Centre Southampton, University of Southampton, Waterfront Campus, European Way, Southampton SO14 3ZH, UK
[b] CSIRO Earth Science and Resource Engineering, 26 Dick Perry Avenue, Kensington, WA 6151, Australia
[c] Geological Survey of Northern Ireland, Dundonald House, Upper Newtownards Road, Belfast BT4 3SB, UK
[d] Department of Earth Sciences, Natural History Museum, London SW7 5BD, UK
[e] School of Biological, Earth & Environmental Sciences, University College Cork, North Mall Campus, Cork, Ireland
[f] Minerex Petrographic Services, P.O. Box 548, Kalgoorlie, WA 6430, Australia
[g] Department of Earth Sciences, Memorial University of Newfoundland, St. John's, NL A1B 3X5, Canada
[h] Aurum Exploration Services, 105 Consumers Drive, Whitby, Ontario L1N 1C4, Canada

ARTICLE INFO

Article history:
Received 29 April 2015
Revised 3 August 2015
Accepted 6 September 2015
Available online 10 September 2015

Keywords:
Iron formation
Ironstone
Jasper
Exhalite
Tuffite
VMS
Grampian
Taconic

ABSTRACT

Iron formations, hematitic cherts (jaspers), 'tuffites', silica-iron exhalites and other metalliferous chemical sedimentary rocks are important stratigraphic marker horizons in a number of volcanogenic massive sulfide (VMS) districts worldwide, forming during episodes of regional hydrothermal activity. The VMS prospective ca. 484–464 Ma Tyrone Igneous Complex of Northern Ireland represents a structurally dissected arc-ophiolite complex that was accreted to the composite margin of Laurentia during the Grampian orogeny (ca. 475–465 Ma), and a potential broad correlative to the VMS-rich Buchans–Robert's Arm arc system of the Newfoundland Appalachians. Silica-iron-rich rocks occur at several stratigraphic levels in the Tyrone Igneous Complex spatially and temporally associated with rift-related basalts (e.g., Fe–Ti-rich eMORB, IAT, OIB) and zones of locally intense hydrothermal alteration. In the ca. 475–474 Ma lower Tyrone Volcanic Group, these rocks are characterized by massive, 1–5 m thick blood-red jaspers, hematitic siltstones and mudstones, and intensely silica-hematite altered tuffs and flows. Their mineralogy is dominated by quartz–hematite ± magnetite–(chlorite-sericite ± tremolite/actinolite), with Fe concentrations rarely exceeding 10 wt.%. Relict textures (including the presence of coalesced spherules of silica-iron oxides) in rocks exposed at Tanderagee NW, Creggan Lough and Tory's Hole are indicative of seafloor exhalation, whereas replacement of the original volcanic stratigraphy is evident to varying degrees at Tanderagee, Beaghbeg and Bonnety Bush. In the structurally overlying ca. 473–469 Ma upper Tyrone Volcanic Group, chemical sedimentary rocks include recrystallized: (i) thin and laterally-restricted jaspers in thick sequences of graphitic pelite at Boheragh; and (ii) laterally-persistent sulfidic cherts and ironstones dominated by quartz–hematite–magnetite–(chlorite) or quartz–pyrite–(chlorite) in sequences of tuff at Broughderg. Compared to chemical sedimentary rocks associated with VMS deposits worldwide, their geochemical characteristics are most similar to silica-iron exhalites of the Mount Windsor Subprovince (SE Australia) and jaspers of Central Arizona, Bald Mountain (Northern Maine), the Urals, Iberian Pyrite Belt and Løkken ophiolite (Norway). Positive Eu anomalies (at Slieve Gallion and Tanderagee NW), elevated Cu + Pb + Zn, Au, Fe/Ti, Fe/Mn, Sb, Ba/Zr and Fe + Mn/Al, together with low REE, Sc, Zr and Th, are indicative of a greater hydrothermal component and potentially more VMS-proximal signatures. Based on bulk ironstone geochemistry, Bonnety Bush, Tanderagee NW-Creggan Lough, Broughderg and Drummuck (Slieve Gallion) are considered the most VMS prospective areas in the Tyrone Igneous Complex and warrant further exploration.

1. Introduction

Iron formations, hematitic cherts (jaspers), 'tuffites', umbers, silica-iron exhalites and other metalliferous chemical sedimentary rocks (e.g., sulfidic cherts and mudstones; Table 1) form important stratigraphic

* Corresponding author at: CSIRO Earth Science and Resource Engineering, 26 Dick Perry Avenue, Kensington, WA 6151, Australia
E-mail address: stevenphiliphollis@gmail.com (S.P. Hollis).

http://dx.doi.org/10.1016/j.gexplo.2015.09.001
0375-6742/

Table 1
Definitions for chemical sedimentary rocks used herein.

Term	Definition	References
Ironstone (sensu stricto)	Sedimentary rock that contains >15 wt.% Fe. Includes: iron formations, metalliferous sediments, Fe–Mn nodules, pavements and crusts.	Stow (2005)
Iron formation	Layered, bedded or laminated rocks with >10 wt.% Fe, where iron minerals are interlayered with quartz, chert or carbonate. Divisible into Superior- and Algoma-types. Referred to as banded iron formation (BIF) in Precambrian terranes.	Gross (1980), Spry et al. (2000), Bekker et al. (2010)
Chert	Fine-grained siliceous sedimentary rock of biogenic, biochemical or chemogenic origin. Composed predominantly of fine-grained silica with small quantities of impurities. Green colors are typically associated with chlorite or smectite clays from volcaniclastics, and dark colors with clays and organic carbon.	Stow (2005)
Hematitic chert/jasper	Red colored chert, with its color imparted by finely disseminated hematite. May be recrystallized or show poikilitic textures with cryptocrystalline hematite dispersed in a silica matrix. Of variable thickness (few cm to >10 m).	Maslennikov et al. (2012)
Sulfidic chert/mudstone	Chert/mudstone with visible sulfide minerals above trace amounts (i.e. >1%).	Defined herein
Iron-rich chert	Chert with a high content of iron oxide minerals and 5–15 wt.% Fe.	
Jaspillite	Interbedded jasper and hematite. Australian term for a banded iron formation (BIF).	Allaby (2013)
Tetsusekiei	Iron quartz in Japanese. Generic name used for silica-iron rich chemical sedimentary rocks of the Kuroko district, Japan. Interpreted as a mixture of both clastic (tuffaceous) and exhalative (chemical) material.	Kalogeropoulos and Scott (1983)
Tuffite (sensu lato)	Generic name used for tuffaceous chemical sedimentary rocks (often referred to as tuffaceous exhalites) in the Abitibi greenstone belt, Canada. Examples: Key Tuffite, Main Contact Tuff.	Kalogeropoulos and Scott (1989)
Tuffite (sensu stricto)	A rock which contains a mixture of pyroclastic (25–75%) and epiclastic material. May be divided according to average clast size into tuffaceous conglomerate/breccias, tuffaceous sandstone, tuffaceous siltstone, and tuffaceous mudstone/shale.	Le Maitre (2004)
Umber (or umbrite)	A sedimentary deposit of Fe–Mn oxyhydroxides admixed with variable amounts of biogenic and detrital material (e.g., chlorite, silica and carbonate) forming trace-metal enriched mudstones.	Maslennikov et al. (2012) and references therein
Ochre	Gossan-derived unmetamorphosed ferruginous sediments (e.g., Semail Nappe and Troodos, Cyprus).	
Jasperite	Orange hematite–quartz rocks differentiated from jaspers on account of microbreccia-like textures and abundant features indicative of replacement inherited from former hyaloclastite. Fragments of fine grained hematite–quartz aggregates are cemented by a blocky quartz matrix. Jasperites can occur as veins, interpillow interstitial infillings, stratiform lenses, beds and interbeds.	
Gossanite	A submarine gossan-derived sedimentary rock and the lithified analogues of ochres. Generally comprise oxidized clastic sulfides mixed with hematitized carbonate and/or hyaloclastic material almost entirely replaced by silica, chlorite and hematite.	
Exhalite	A unit formed through precipitation of mainly amorphous Fe ± Mn ± Si ± S ± Ba ± B phases from VMS-related hydrothermal vents and plumes at or below the seafloor.	Peter and Goodfellow (1996, 2003), Grenne and Slack (2005), Slack (2012)
Vasskis	Beds of silicate- and sulfide-facies iron formation in Norway (e.g., Løkken district).	Slack (2012)

horizons in a number of volcanogenic massive sulfide (VMS) districts worldwide. These units often mark the most prospective sequences for mineralization and can occur stratigraphically above, below, in, or along strike from orebodies (Galley et al., 2007; Kalogeropoulos and Scott, 1983, 1989; Leistel et al., 1998; Peter, 2003; Peter and Goodfellow, 1996; Spry et al., 2000). Classic examples include the tetsusekiei (iron quartz) of the Fukazawa Mine, Japan (Kalogeropoulos and Scott, 1983; Tsutsumi and Ohmoto, 1983); 'tuffites' of the Abitibi greenstone belt, Canada (Genna et al., 2014a; Kalogeropoulos and Scott, 1989; Liaghat and MacLean, 1992); jasperites, gossanites and umbers of the Urals (Herrington et al., 2005; Maslennikov et al., 2012); and iron formations of the Brunswick Horizon of the Bathurst Mining Camp, Canada (Peter and Goodfellow, 1996).

Based on interpreted depositional settings, silica-iron-rich chemical sedimentary rocks were originally divided into two groups by Gross (1980, 1983): Algoma- and Superior-type iron formations. Although Algoma-type iron formations are mineralogically similar to Superior-type iron formations, the former are volcanic-hosted, deep-water and commonly associated with VMS mineralization (Bekker et al., 2010; Slack et al., 2007). Algoma-type iron formations form in volcanic arcs, backarcs, spreading ridges and rifts, and have been interpreted by a number of workers to precipitate from the venting of hydrothermal fluids contemporaneous with volcanism (Peter, 2003; Slack et al., 2007). Jaspers form as silica-iron gels, precipitated from the non-buoyant parts of hydrothermal plumes; ferrous iron is oxidized to insoluble ferric iron oxyhydroxides, which in turn promotes the flocculation of seawater-derived amorphous silica (Slack et al., 2007). Deposits of silica-rich iron oxyhydroxides have been documented on the modern seafloor associated with a number of hydrothermal systems (German et al., 1993; Halbach et al., 2002; Hekinian et al., 1993; Juniper and Fouquet, 1988), although many of these are laterally restricted (Grenne and Slack, 2003). Superior-type iron formations, by contrast, are characterized by interlayered chert and iron oxides in shallow-water sedimentary sequences (Slack et al., 2007). As these rocks are not associated with VMS-mineralization, they are not discussed further.

The Caledonian–Appalachian orogenic belt (Fig. 1A) hosts significant VMS mineralization along its length from Quebec, through New Brunswick and Newfoundland (Piercey, 2007; van Staal, 2007), into Ireland (e.g., Avoca; McConnell et al., 1991), Great Britain (e.g., Parys Mountain; Colman and Cooper, 2000; Barrett et al., 2001) and Scandinavia (Grenne and Vokes, 1990; Grenne et al., 1999). The ca. 484–464 Ma Tyrone Igneous Complex of Northern Ireland (Fig. 1B), a structurally dissected arc-ophiolite complex, has been a target for base and precious metal exploration since the early 1970s (Clifford et al., 1992; Leyshon and Cazalet, 1978; Peatfield, 2003). Recently established temporal, lithological and geochemical similarities with the VMS-rich Buchans–Robert's Arm arc system of central Newfoundland (Cooper et al., 2011; Hollis et al., 2012, 2013a; see Table 2), indicate that the Tyrone Igneous Complex is prospective for VMS mineralization (Hollis et al., 2014, in press). The Buchans–Robert's Arm belt hosts high-grade Kuroko-type VMS deposits at Buchans (16.2 Mt mined at 14.51% Zn, 7.56% Pb, 1.33% Cu, 126 g/t Ag and 1.37 g/t Au: Thurlow, 2010), as well as smaller Cyprus-type and Noranda-type deposits elsewhere (Piercey and Hinchey, 2012; van Staal et al., 2007). Stratigraphic horizons have been identified in the Tyrone Igneous Complex that are prospective for VMS mineralization, characterized by rift-related mafic flows (e.g., IAT, eMORB), geochemically 'fertile' felsic rocks (i.e. indicative of melting at shallow levels and elevated crustal heat flux; after Lesher et al., 1986; Hart et al., 2004), zones of locally intense hydrothermal alteration, base and precious metal occurrences, geophysical anomalies, and in some instances

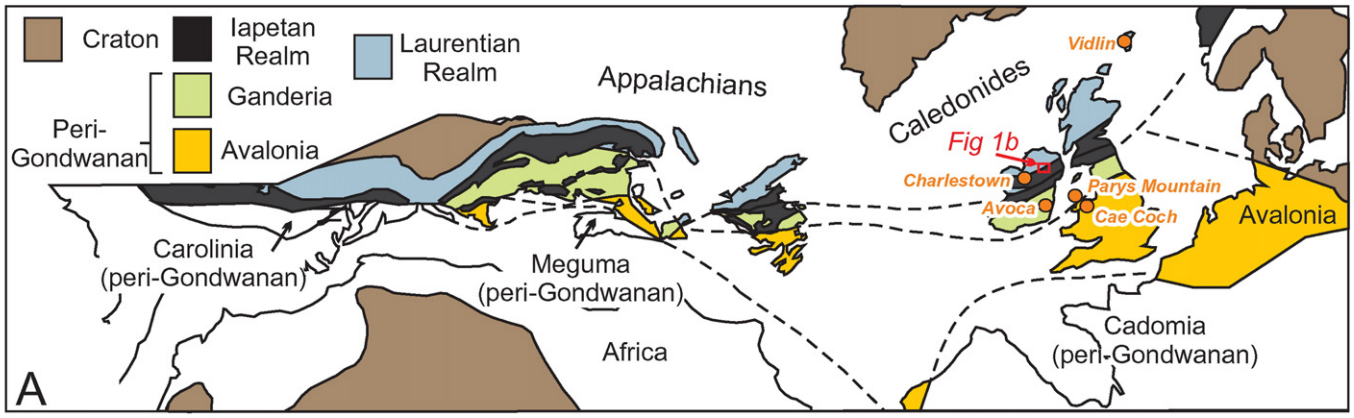
Craton
Iapetan Realm
Laurentian Realm
Ganderia
Peri-Gondwanan
Avalonia
Appalachians
Caledonides
Vidlin
Fig 1b
Charlestown
Parys Mountain
Avoca
Cae Coch
Avalonia
Carolinia (peri-Gondwanan)
Meguma (peri-Gondwanan)
Africa
Cadomia (peri-Gondwanan)
A

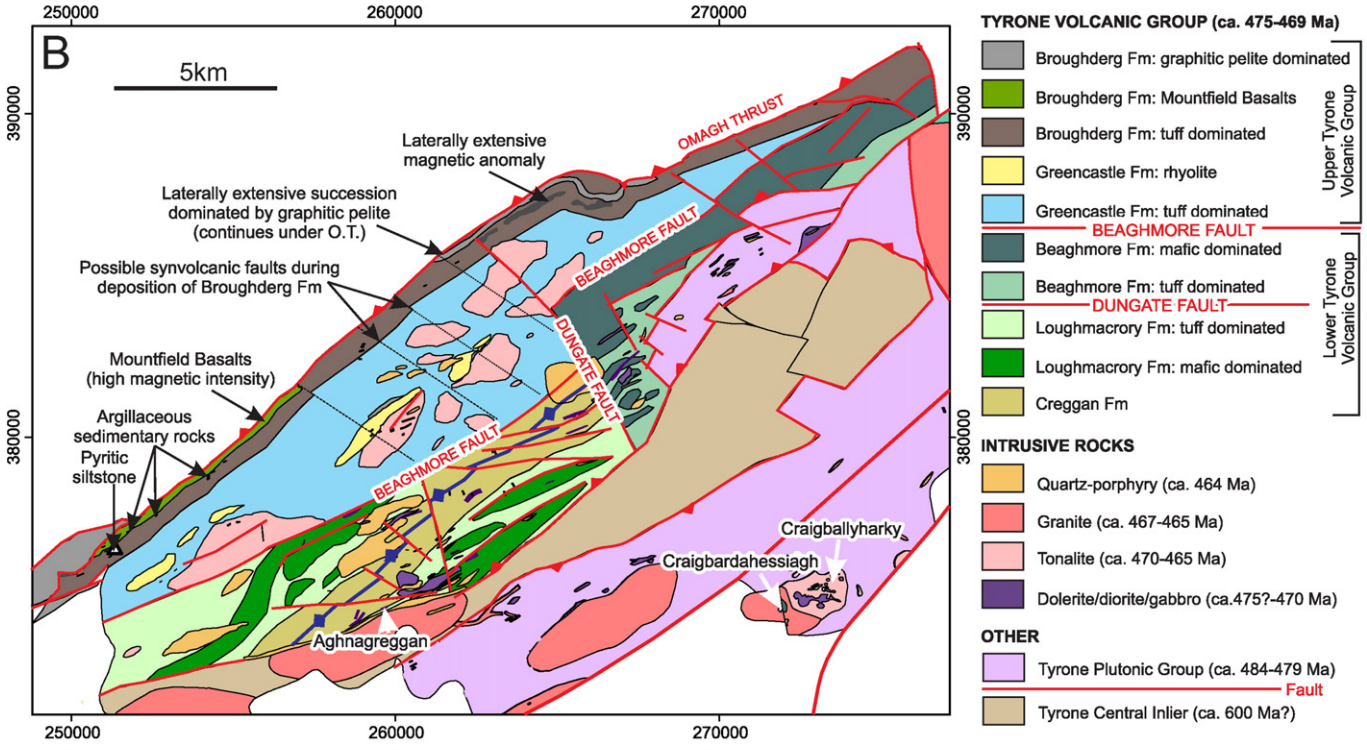
B
5km
250000
260000
270000
390000
380000
Laterally extensive magnetic anomaly
OMAGH THRUST
Laterally extensive succession dominated by graphitic pelite (continues under O.T.)
BEAGHMORE FAULT
Possible synvolcanic faults during deposition of Broughderg Fm
DUNGATE FAULT
Mountfield Basalts (high magnetic intensity)
Argillaceous sedimentary rocks
Pyritic siltstone
BEAGHMORE FAULT
Craigballyharky
Craigbardahessiagh
Aghnagreggan
TYRONE VOLCANIC GROUP (ca. 475-469 Ma)
Broughderg Fm: graphitic pelite dominated
Broughderg Fm: Mountfield Basalts
Broughderg Fm: tuff dominated
Greencastle Fm: rhyolite
Greencastle Fm: tuff dominated
Upper Tyrone Volcanic Group
BEAGHMORE FAULT
Beaghmore Fm: mafic dominated
Beaghmore Fm: tuff dominated
DUNGATE FAULT
Loughmacrory Fm: tuff dominated
Loughmacrory Fm: mafic dominated
Creggan Fm
Lower Tyrone Volcanic Group
INTRUSIVE ROCKS
Quartz-porphyry (ca. 464 Ma)
Granite (ca. 467-465 Ma)
Tonalite (ca. 470-465 Ma)
Dolerite/diorite/gabbro (ca.475?-470 Ma)
OTHER
Tyrone Plutonic Group (ca. 484-479 Ma)
Fault
Tyrone Central Inlier (ca. 600 Ma?)

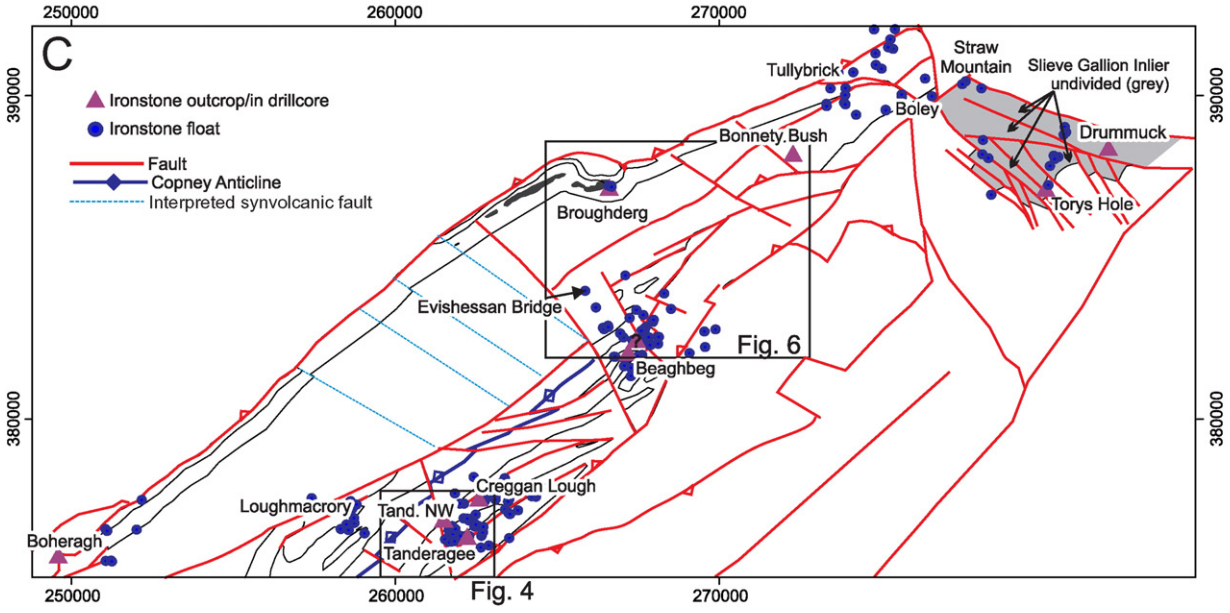
C
250000
260000
270000
390000
380000
Ironstone outcrop/in drillcore
Ironstone float
Fault
Copney Anticline
Interpreted synvolcanic fault
Tullybrick
Straw Mountain
Slieve Gallion Inlier undivided (grey)
Boley
Bonnety Bush
Drummuck
Broughderg
Torys Hole
Evishessan Bridge
Fig. 6
Beaghbeg
Creggan Lough
Loughmacrory
Tand. NW
Tanderagee
Boheragh
Fig. 4

Table 2
Comparison between the VMS-rich Annieopsquotch Accretionary Tract of Newfoundland, Canada, and the Tyrone Igneous Complex, Northern Ireland. Data sources: Tyrone Igneous Complex (Chew et al., 2008; Cooper et al., 2008, 2011; Draut et al., 2009; Hollis et al., 2012, 2013a, 2013b, 2014; Hutton et al., 1985), Annieopsquotch Accretionary Tract (after Dunning and Krogh, 1985; Zagorevski, 2008; Zagorevski and van Staal, 2011; Zagorevski et al., 2006, 2008, 2014). BABB, backarc basin basalt; CAB, calc-alkaline basalt; eMORB, enriched mid ocean ridge basalt; IAT, island arc tholeiite; OIB, ocean island basalt.

		Annieopsquotch Accretionary Tract, Newfoundland, Canada	Tyrone Igneous Complex, Northern Ireland
Affinity		Laurentian	Laurentian
Suprasubduction zone ophiolite	Name	Annieopsquotch Ophiolite Belt	Tyrone Plutonic Group
	Age	481.4 + 4.0/−1.9 to 477.5 + 2.6/−2.0 Ma	483.68 ± 0.81 to 479.6 ± 1.1 Ma
	Preserved lithologies	Layered, isotropic and pegmatitic gabbros, sheeted dykes and pillow lavas. Lesser felsic intrusive rocks (e.g., at Moretons Harbour).	Layered, isotropic and pegmatitic gabbros, sheeted dykes, rare pillow lavas. Rare plagiogranite and tuff.
	Minor crustal inheritance	T_{DM} ages of 1200–1800 Ma in felsic intrusive rocks	Rare Proterozoic zircons and low εNd_t values (+4.5 to +7.5)
	Preserved mantle section?	Rare and isolated small bodies of dunite and pyroxenite	Possible pyroxene-rich ultramafic fragments
	Geochemical affinity	IAT with late nMORB and BABB	IAT
Island arc(s)	Name	Robert's Arm and Buchans groups	Tyrone Volcanic Group
	Age	ca. 473 & 464 Ma respectively	ca. 475 to >469 Ma (uppermost concealed)
	Geochemical affinity	Basalt: CAB, IAT. Fe–Ti basalt? Rhyolite: Calc-akaline FII type, lesser tholeiitic	Basalt: CAB, Fe–Ti eMORB, lesser IAT, OIB and alkali-basalt Rhyolite: Calc-alkaline FII type, lesser M-type tholeiitic and A-type high Zr.
	Arc type	Oceanic to continental plus backarc Built on fragment of microcontinental crust	Oceanic to continental plus backarc Built on fragment of microcontinental crust(?)
	Rifting type	Disorganized spreading	Disorganized spreading
Synvolcanogenic diorite and/or tonalite		ca. 470 Ma	ca. 470 to 465(?) Ma
Late granitic intrusive rocks		ca. 467 Ma(?) e.g., Wileys Brook	ca. 467 to 464 Ma
Accreted to		Dashwoods Block Outboard microcontinental block Peri-Laurentian	Tyrone Central Inlier Outboard microcontinental block(?) Peri-Laurentian
Timing of accretion		ca. 473 to 468 Ma (for ca. 473 Ma arc)	ca. 473 to 470 Ma.
VMS mineralization		Dominantly: Kuroko type (e.g., high grade Buchans deposits: 16.2 Mt mined). Lesser: Cyprus type (e.g., Skidder deposit 0.2 Mt at 2% Cu, 2% Zn) & Noranda type (e.g., Gullbridge 3 Mt at 1.1% Cu)	Kuroko-type prospects (upper arc). Some Cyprus type (ophiolite-hosted) and Noranda type prospects (lower arc).

silica-iron-rich sedimentary rocks (the ironstones — sensu lato — of Cooper and Mitchell, 2004; Cooper et al., 2011; Hollis et al., 2012, 2014, in press; Fig. 1C).

The geochemical characteristics of iron formations and other chemical sedimentary rocks associated with VMS deposits may be used as an inexpensive tool for regional mineral exploration (Carvalho et al., 1999; Davidson et al., 2001; Kalogeropoulos and Scott, 1983; Miller et al., 2001; Peter, 2003; Peter and Goodfellow, 1996). The relative abundance of certain minerals (e.g., iron carbonates, apatite, gahnite, Zn-rich staurolite), whole rock geochemical compositions (Eu/Eu*, Fe/Ti, Cu + Pb + Zn, Tl, Sb), mineral chemical variations (e.g., Fe/Mg in chlorite) and stable isotope compositions (S, C, O, and B) have been shown to serve as useful vectors to VMS mineralization across certain districts/camps (reviewed in Spry et al., 2000; Peter, 2003; see Fig. 2). This paper presents the first study of these silica-iron-rich rocks in Northern Ireland, and discusses their distribution, mineralogy and geochemical characteristics in relation to VMS-associated units worldwide. Geochemical vectors to mineralization (after Peter and Goodfellow, 1996; Spry et al., 2000; Peter, 2003) are used to identify the most prospective areas for exploration.

2. Classification of chemical sedimentary rocks

As outlined above, the scientific literature contains myriad terms for different types of silica-iron-rich chemical sedimentary rocks associated with ancient VMS mineralization and modern seafloor hydrothermal activity. These include: Algoma-type iron formations, hematitic cherts (jaspers), jasperites, gossanites, umbers, ochres, 'tuffites', exhalites, ironstones, sulfidic cherts and mudstones, tetsusekiei ('iron quartz' in Japanese), vasskis. The work herein follows the definitions outlined in Table 1. The term ironstone (sensu stricto) should only be used for chemical sedimentary rocks where there is >15 wt.% Fe. Two units of the Tyrone Igneous Complex meet this criterion, at least locally along their strike length, based on bulk whole rock geochemical data — the unit exposed at Bonnety Bush and a unit intercepted by recent diamond drilling at Broughderg (Fig. 1C). Although many other units may grade to ironstone, exposure is poor and geochemical data are limited. Consequently, apart from the limited true ironstones, the silica-iron-rich rocks in the Tyrone Igneous Complex are herein referred to as jaspers, Fe-rich cherts and sulfidic cherts based on petrographic characteristics and whole rock geochemical data. Several units are also interpreted to be exhalites (see discussion).

3. Distribution and field relationships of silica-iron-rich rocks

The Tyrone Igneous Complex (Fig. 1B) is exposed over ca. 350 km^2 of the counties of Tyrone and Londonderry, Northern Ireland, and is interpreted to be an arc-ophiolite complex that was accreted to the Laurentian margin during the Ordovician (Cooper and Mitchell, 2004; Cooper et al., 2008; Draut et al., 2009; Hutton et al., 1985). The ca. 484–479 Ma Tyrone Plutonic Group forms the structurally lowest levels of the complex and preserves a tectonically dissected suprasubduction

Fig. 1. (A) Early Mesozoic restoration of the North Atlantic region and Caledonian–Appalachian orogen (after Pollock et al., 2009), with the position of VMS deposits in the British and Irish Caledonides highlighted (after Hollis et al., 2014). (B) Geological map of the Tyrone Igneous Complex (modified after Hollis et al., 2012, 2014). Possible synvolcanic faults are identified based on the termination of stratigraphic units along strike. Ages after: Draut et al. (2009); Cooper et al. (2008, 2011); Hollis et al. (2012, 2013a, 2013b). Coordinates are Irish grid (in meters). (C) Distribution of ironstone (sensu lato) outcrop and float in the Tyrone Igneous Complex.

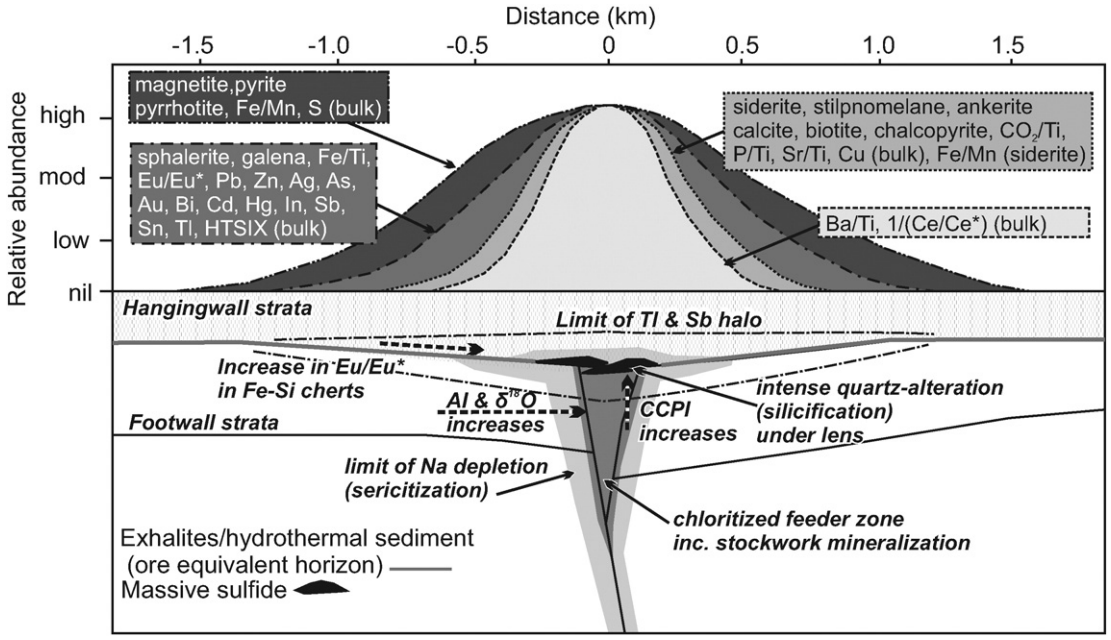

Fig. 2. Schematic diagram showing the lateral extent of mineral, mineral chemical and bulk geochemical halos that surround VMS deposits in the Bathurst Mining Camp (after Peter and Goodfellow, 1996, 2003; Goodfellow, 2007).

zone ophiolite, that has been obducted onto an outboard micro-continental block (the Tyrone Central Inlier: Chew et al., 2008) prior to ca. 470 Ma (Cooper et al., 2011; Draut et al., 2009; Hollis et al., 2013a; Hutton et al., 1985). The structurally overlying ca. 475–469 Ma Tyrone Volcanic Group (TVG) includes mafic to felsic flows and tuffs, bedded chert, fine grained sedimentary rocks such as siltstone and mudstone, and silica-iron-rich rocks at several stratigraphic levels (the ironstones – sensu lato – of Cooper and Mitchell, 2004; Cooper et al., 2008, 2011; Hollis et al., 2012, 2013b, 2014, in press). Geochemical signatures are consistent with their formation in an evolving peri-Laurentian island arc/backarc which underwent several episodes of extension (Hollis et al., 2012, 2014). Rift-related magmatism is characterized by the presence of enriched-mid ocean ridge basalt (eMORB), island arc tholeiitic basalt (IAT) and low-Zr tholeiitic rhyolite in the lower Tyrone Volcanic Group; and by ocean island basalt (OIB), alkali basalt and high-field strength element (HFSE) enriched rhyolite in the upper Tyrone Volcanic Group (Hollis et al., 2012, 2014; Fig. 3). Both the Tyrone Volcanic Group and Tyrone Plutonic Group are intruded above the Tyrone Central Inlier by a suite of high-level and arc-related tonalitic to granitic rocks (ca. 470–464 Ma) (Cooper and Mitchell, 2004; Draut et al., 2009; Cooper et al., 2011; Fig. 1B). The Proterozoic Dalradian Supergroup was subsequently thrust over all of these units during regional deformation (Alsop and Hutton, 1993), with the two terranes separated by the Omagh Thrust (Fig. 1B).

Despite being volumetrically rare in the Tyrone Igneous Complex, silica-iron-rich rocks occur in all three structural blocks of the Tyrone Volcanic Group (E, NW and SW), in three of five formations (Loughmacrory, Beaghmore, Broughderg: Hollis et al., 2012), as roof pendants in the Craigbardahessiagh intrusion (Cobbing et al., 1965), and in the volcanic succession exposed on Slieve Gallion (Hollis et al., 2013b; Figs. 1C, 3). Although the rocks exposed on the eastern side of the Tyrone Volcanic Group at Tanderagee, Beaghbeg and Bonnety Bush (Fig. 1C) have previously been interpreted to represent a single unit (Cobbing et al., 1965), more recent work has demonstrated that they occur at different stratigraphic levels, spatially and temporally associated with rift-related magmatism (Cooper and Mitchell, 2004; Cooper et al., 2011; Hollis et al., 2012, 2014; Fig. 3). Field relationships are summarized below, with additional detail provided in Table 3. Field localities discussed herein (Fig. 1C) are named after local town lands and features on 1:50,000 scale ordinance survey maps, consistent with previous stratigraphic work on the complex (e.g., Cooper and Mitchell, 2004; Cooper et al., 2008, 2011; Hollis et al., 2012, 2013b). Metamorphic grade in the Tyrone Volcanic Group is predominantly subgreenschist, with greenschist facies rocks exposed closest to the Omagh Thrust (Fig. 1B).

3.1. Lower Tyrone Volcanic Group

The lower Tyrone Volcanic Group, exposed south of the Beaghmore Fault, is divided into three formations: Creggan, Loughmacrory, Beaghmore (Hollis et al., 2012; Fig. 1B). There are no U–Pb zircon geochronologic data for this part of the sequence; its age (ca. 475–474 Ma: Cooper et al., 2008) is based on stratigraphic and geochemical correlations with the graptolite-bearing volcanic succession at Slieve Gallion (Hollis et al., 2013b; Fig. 3). In the lower Tyrone Volcanic Group, 1–5 m thick massive blood-red jaspers, hematitic metasedimentary rocks (siltstones and mudstones), and gray silica-iron-rich rocks of tuffaceous appearance, occur in the Loughmacrory and Beaghmore formations (Figs. 1B, 3; see Table 3). Rare clasts of jasper also occur within basaltic breccias of eMORB-affinity in the underlying Creggan Formation (Hollis et al., 2012). Massive and layered, Fe-poor, gray cherts are present in both the Creggan and Loughmacrory formations, but these are not discussed further (see Hollis et al., 2012 for bulk geochemical data).

3.1.1. Loughmacrory formation

Although several localities in the Loughmacrory Formation contain abundant silica-iron-rich float, outcrops are rare (Fig. 1C). On the Geological Survey of Northern Ireland 1:50,000 Pomeroy sheet (Geological Survey of Northern Ireland, GSNI, 1979), a NE–SW trending red to blue–black hematite-rich ironstone (sensu lato: Tanderagee Siliceous Ironstone Member) was mapped at two localities — Tanderagee and Aghnagreggan (Figs. 1B, 4). Additional outcrops occur at Creggan Lough and Tanderagee NW (Figs. 1C, 4; Table 3). The Aghnagreggan and Tanderagee NW exposures represent the stratigraphically lowest silica-iron-rich rocks identified in the Tyrone Volcanic Group. Both units crop out near rift-related flows of Fe–Ti-rich eMORB affinity along the SE margin of the Creggan Formation (Figs. 1B, 4). At

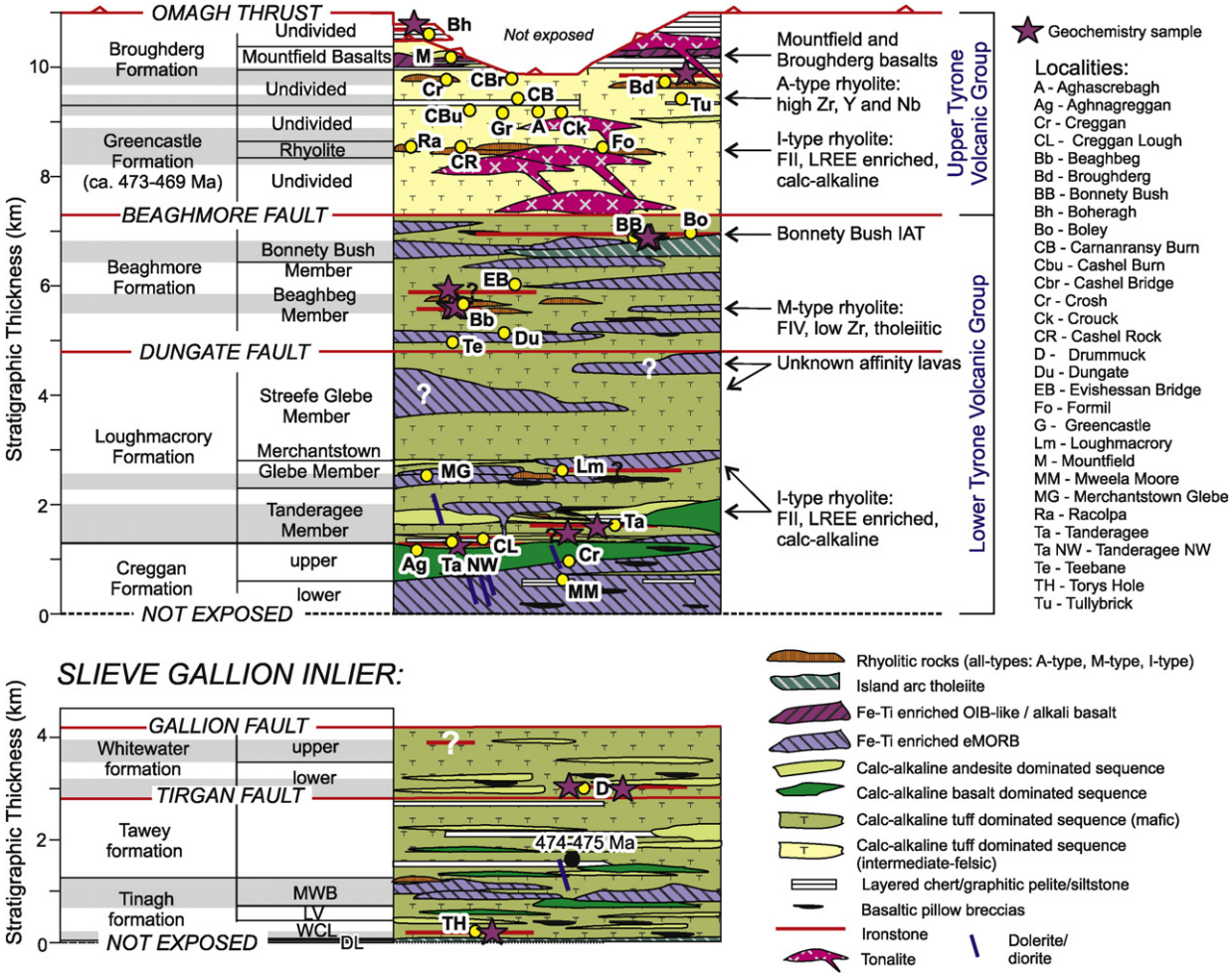

Fig. 3. Simplified stratigraphic section for the Tyrone Volcanic Group and Slieve Gallion Inlier (after Hollis et al., 2013b, 2014) showing the geochemical affinity of different units. Gray shading reflects the VMS-prospective stratigraphic horizons identified in Hollis et al. (2014). DL, Derryganard Lavas; LV, Letteran Volcanics; MWB, Mobuy Wood Basalts; WCL, Windy Castle Lavas.

Tanderagee NW, pale red jasper is exposed for ~2 m (Fig. 5A) adjacent to a sequence of tuffaceous, blue–gray chert. Jasper is typically massive and dominated by quartz–hematite, with magnetite present on discontinuities and associated with quartz veinlets/brecciation (Table 3). Internally these rocks are characterized by rounded (to locally angular) blebs of blood-red jasper set in a darker gray quartz-rich matrix.

Stratigraphically higher in the Loughmacrory Formation, jasper float, which locally contains 5–10% finely disseminated and stringer pyrite, is common around Creggan Lough (Fig. 4). Float is similar in appearance to the jasper exposed at Tanderagee NW (Table 3). Higher still in the stratigraphy at Tanderagee, a maroon to blood-red hematitic mudstone crops out adjacent to vesicular calc-alkaline basalt and late quartz-feldspar porphyry (Fig. 5B; Table 3). Minor quartz veining and pyrite occur in the outcrop. Abundant blood-red, silicified and quartz-veined jasper float occurs along strike of the mapped unit (Fig. 5C) coincident with a series of Tellus airborne electromagnetic (EM) anomalies (Fig. 4).

3.1.2. Beaghmore formation

In the Beaghmore Formation, silica-iron-rich rocks crop out at Beaghbeg and Bonnety Bush (Figs. 1C, 6). At Beaghbeg, a 3 to 5 m wide blood red to pale gray unit, dominated by quartz–hematite ± magnetite, is intermittently exposed for ~20 m along strike (Fig. 5D–G; see Table 3). Stratigraphically higher in the Beaghmore Formation at Bonnety Bush (Fig. 3), a >4 m thick unit of ironstone forms a low rise on a flat glacial outwash plain (Fig. 7) and is intermittently exposed for at least 70 m along strike. Both units are extremely variable in appearance and have a similar genesis (see following). At both localities early blood-red domains of silica-hematite (that resemble jasper) are brecciated by a darker red variety of silica-hematite, cut by fine white quartz veinlets. At Bonnety Bush the blood-red rock which resembles jasper crops out at the SE end (Fig. 7A–B), with intense silicification concentrated towards the central section (Fig. 7C–E). At the NE end of the Bonnety Bush exposures the unit becomes increasingly tuffaceous in appearance and brecciated by chlorite–magnetite. As at Beaghbeg, fine magnetite–chlorite-forms a matrix to early formed large angular blocks dominated by quartz–hematite (Fig. 7F), which is in turn cut by late veins of quartz (Fig. 7G) and a younger set of NW–SE striking quartz veins which contain platy Fe-oxides (Fig. 7H). Geophysical data from the Tellus regional magnetic survey of Northern Ireland (Young and Donald, 2013) has revealed that the Bonnety Bush exposures lie along one of several prominent magnetic highs that extend for several kilometers along strike (Fig. 6).

3.1.3. Slieve Gallion Inlier

At Tory's Hole, in the ca. 475–474 Ma Slieve Gallion Inlier (Fig. 1C), a 1–5 m thick, bed of massive and blood-red jasper is exposed in a small stream section towards the base of the Tinagh Formation (Hollis et al., 2013b; Fig. 3). This NW–SE striking unit comprises small (<0.5 cm) fragments of blood-red jasper brecciated by a matrix of silica-hematite, cut by quartz veins. No contacts to adjacent units are exposed. The lower part of the Tinagh Formation is dominated by mafic to

Table 3
Field characteristics and stratigraphic relationships for silica-iron rich rocks from the Tyrone Igneous Complex.

Area & Irish grid	Formation & age	Local stratigraphy	Appearance
Aghnagreggan 259645E-374770N	Loughmacrory; ca. 475–474 Ma	Adjacent to Fe–Ti eMORB lavas of the Creggan Formation. Along strike from the Tanderagee NW outcrop.	Jasper/ironstone float was not located during recent fieldwork.
Tanderagee NW 261279E-376954N		Adjacent to blue–gray chert near mapped extent of the Creggan Formation. Stratigraphically overlying exposures of the Tanderagee Member include: sandstone, layered cream–gray–black colored chert exhibiting soft-sediment deformation features, polymict volcanic breccias, ophitic basalt of FeTi eMORB affinity, black chert and basaltic tuff, and fine grained metasedimentary rocks (siltstone and chert) interbedded with tuff.	Siliceous and pale red jasper crops out for ~2 m (Fig. 5A). Jasper float is massive and dominated by quartz–hematite, with magnetite present on fractures and associated with quartz veinlets/brecciation. Internally these rocks are characterized by rounded (to locally angular) blebs of blood-red jasper set in a grayer and darker quartz matrix.
Creggan Lough 262616E-377529N		Jasper float only. Historic outcrops lost. Calc-alkaline tuffs and mafic-intermediate lavas of the Loughmacrory Formation. Tellus geophysics data (Young and Donald, 2013) reveals a weak magnetic high in the area, but it is unclear if this reflects this unit or a continuation of the Granagh Basalts (Fig. 4).	Blood red jasper with up to 10% finely disseminated pyrite. Otherwise identical to description from Tanderagee NW.
Tanderagee 262205E-376330N		Descriptions of the contacts by Hutton (1983) state the northeast contact is against a younger intrusion of quartz-porphyry (dated elsewhere in the Tyrone Volcanic Group to 465.0 ± 1.7 Ma: Cooper et al., 2011) and the southwest contact is against vesicular mafic lava of calc-alkaline affinity.	Maroon to blood-red hematite altered mudstone/fine grained tuff. Minor quartz veining, sulfides and chlorite–magnetite brecciation also occurs in the outcrop (Fig. 5B).
Beaghbeg 267463E-382492N	Beaghmore; ca. 475–474 Ma	Surrounding lithologies include silicified and hematite-altered tuffs, and low-Zr tholeiitic rhyolite breccias which can contain rare <5 cm angular fragments of the underlying rocks. Jasper-like fragments also occur in the stratigraphically overlying sequence at Balloughtragh and as <30 cm thick quartz–hematite veins which locally cross-cut sequences of tuff. Fe–Ti eMORB lavas crop out further south.	A 3 to 5 m wide blood red to pale gray unit, dominated by quartz–hematite ± magnetite, is intermittently exposed for ~20 m along strike (Fig. 5D–G). Internally the unit is characterized by early blood-red 'jasper', brecciated by a darker red variety of silica-hematite, cut by fine white quartz veinlets. A younger generation of quartz–magnetite veins are in turn brecciated by thick zones of magnetite–chlorite, and the latter are cut by NW–SE striking veins of quartz and coarse gray platy Fe-oxides. Magnetite is also present on fractures.
Bonnety Bush 272243E-388152N		Underlying rocks are poorly exposed, with rare outcrops of silica-epidote altered island-arc tholeiitic basalt. Overlying exposed rocks include tholeiitic and calc-alkaline tuffs.	A >4 m thick unit (Fig. 6) is intermittently exposed for at least 70 m along strike. The rock is massive, blood-red and resembles recrystallized jasper at its SE end (Fig. 7A–B). Silicification and disseminated pyrite (to 1 cm, euhedral) is concentrated towards the central section (Fig. 7C–E). Towards its NE end the unit becomes increasingly tuffaceous in appearance and is brecciated by chlorite–magnetite. As at Beaghbeg, fine magnetite–chlorite-forms a matrix to early formed large angular blocks dominated by quartz–hematite (Fig. 7F), which is in turn cut by late veins of quartz (Fig. 7G) and a younger set of NW–SE striking quartz veins which contain platy Fe-oxides (Fig. 7H).
Broughderg 266600E-387100N	Broughderg; ca. 469 Ma	Occurs within intensely chloritized tuffs which underlies a >70 m thick sequence of variably silicified and quartz-veined graphitic pelite. Surrounding chloritized tuffs contain 1–2 mm magnetite crystals for 35 m above and 20 m below the ironstone. Thin A-type felsic rocks were noted in historic drillcore.	~1.5 m thick and strongly recrystallized. Varies from: gray sulfidic chert (containing finely-laminated bands of pyrite; Fig. 5J) to quartz-veined, gray–blue chert cut by late veinlets of euhedral pyrite (Fig. 5J) to finely-laminated (mm-scale) red–brown–black ironstone characterized by quartz–hematite–magnetite (Fig. 5K).
Boheragh 249598E-375747N		Graphitic pelite dominated sequence, with thin tuffaceous bands.	A thin (20–30 cm) jasper horizon is exposed over ~1 m in an overgrown stream section. A fine layering is present between quartz–hematite and thin bands of carbonaceous material (Fig. 5I). Small (0.5–2 cm) fragments of jasper also occur in adjacent exposures of intensely silicified and quartz-veined pelite breccias.
Torys Hole 280026E-387055N	Tinagh — Slieve Gallion; ca. 475–474 Ma	Poorly exposed. Mafic to intermediate pillow lavas and tuffs.	1–5 m thick, massive and blood-red jasper. This NW–SE striking unit comprises small (<0.5 cm) fragments of blood-red jasper brecciated by a matrix of silica-hematite, again cut by quartz veins. Magnetite is present on discontinuities and in vugs with quartz.
Drummuck 282018E-388514N	Whitewater — Slieve Gallion >ca. 474 Ma	Thick sequence of calc-alkaline tuffs and sheared andesitic lavas.	1 – 5 m thick, NW–SE striking unit extends laterally for at least 60 m. The top surface is characterized by a crust of honeycomb, dark gray and patchy red botryoidal hematite (Fig. 5H).
Craigbardahessiagh 271887E-374738N	N/A	Roof pendant in ca. 464 Ma Craigbardahessiagh granodiorite.	A roof pendant of dark gray to black, glassy, magnetite-rich chert (Fig. 5L) is poorly exposed for ~50 m. Angular 1–3 cm siliceous xenoliths occur in some boulders (Fig. 5L).

intermediate tuffs and pillowed flows (Hollis et al., 2013b). A second outcropping unit in the Slieve Gallion Inlier occurs in a stream section at Drummuck (Fig. 1C) in the younger (<474 Ma) Whitewater Formation (Hollis et al., 2013b; Fig. 5H). This NW–SE striking, 1–5 m thick unit extends laterally for at least 60 m and occurs in a sequence of sheared and hydrothermally altered andesitic flows and tuffs (Table 3).

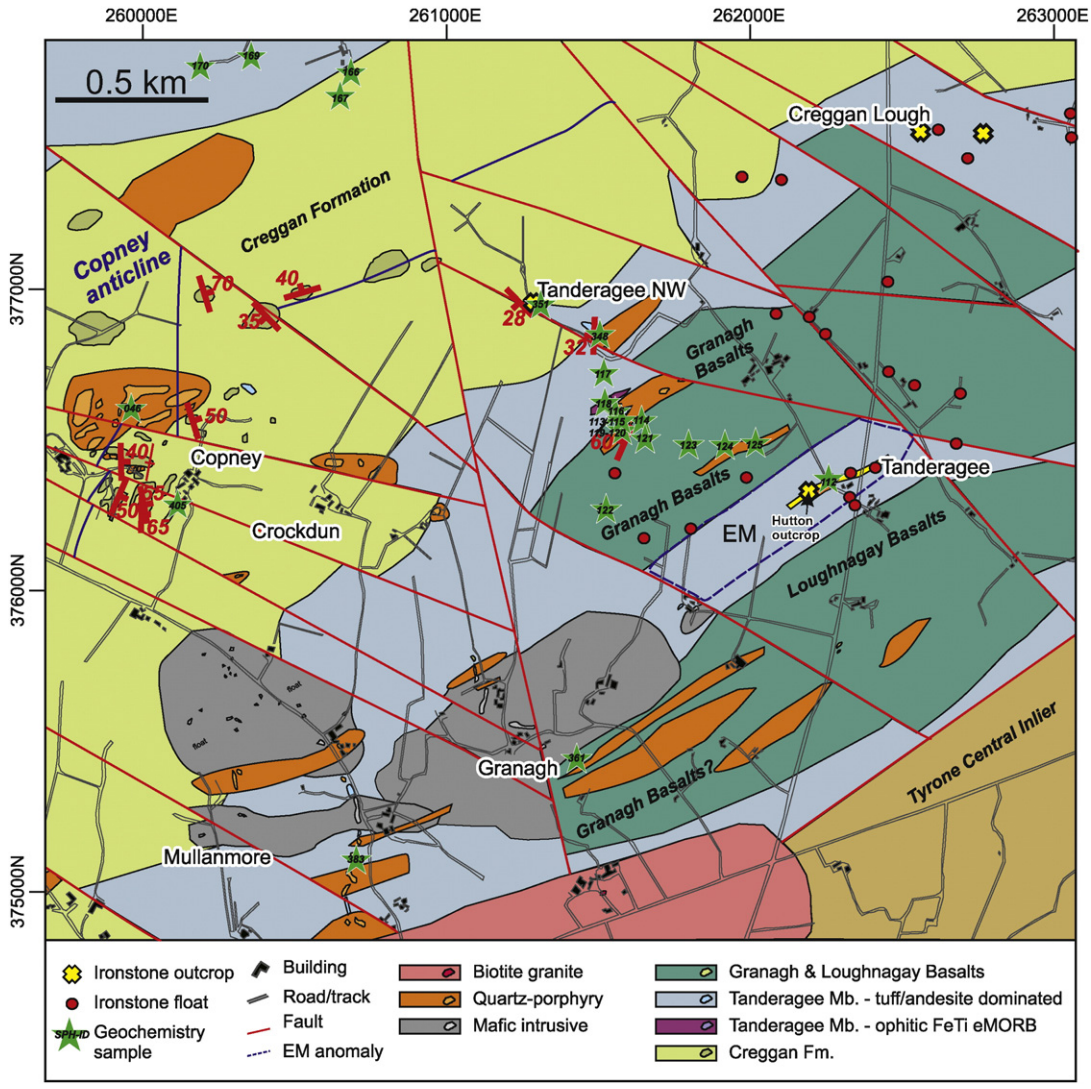

Fig. 4. Geological map of the Tanderagee–Copney area, lower Tyrone Volcanic Group, based on recent mapping. Coordinates are Irish grid.

3.2. Upper Tyrone Volcanic Group

The upper Tyrone Volcanic Group (ca. 473–469 Ma), is a bimodal-felsic succession exposed north of the Beaghmore Fault (Fig. 1B). It includes two formations (Greencastle and Broughderg), and records the accretion of the Tyrone arc to the Tyrone Central Inlier and late (i.e., post-obduction) ensialic arc rifting represented by ca. 469 Ma alkali basalts and HFSE-enriched felsic rocks (Hollis et al., 2014). In the upper Tyrone Volcanic Group, silica-iron-rich rocks are restricted to the Broughderg Formation at Boheragh and Broughderg (Fig. 1C). Hartley (1933) also described small lenticles of chert partly replaced by jasper in Glenscollip Burn (~4 km NE of Boheragh: Fig. 1C), but these rocks were not located during recent fieldwork (Hollis, 2013).

At Boheragh (Fig. 1C), a thin (20–30 cm) jasper horizon is exposed over ~1 m in an overgrown stream section dominated by sheared, graphitic pelite. As these rocks occur in a fault-bound package near the Omagh Thrust (Figs. 1C, 3), it is unclear whether they form part of the uppermost ca. 469 Ma Tyrone Volcanic Group or the Glengawna Formation of the overthrust Proterozoic Dalradian Supergroup. Due to the presence of thin tuffaceous units within the sequence and thick sequences of graphitic pelite along strike at Mountfield and Broughderg, the Boheragh sequence was included as part of the uppermost Tyrone Volcanic Group stratigraphy by Hollis et al. (2012) (Fig. 3). Atypical of the other units of the Tyrone Igneous Complex, a fine banding is present between layers of quartz–hematite and carbonaceous material (Fig. 5I).

At Broughderg (Fig. 1C), ironstone was originally identified during prospecting by Ennex International during the 1980s. Boulders of gray sulfidic and Fe-rich chert locally contain fine bands of pyrite (Fig. 5J). Of five historic trenches cut in the Broughderg area, one intersection contained significant Au (1.5 m at 4.36 g/t: Ennex, 1987). Shallow drilling completed shortly thereafter obtained an intercept of 0.62 m at 1.68 g/t Au (DDH 91-1), associated with a recrystallized and quartz-veined, gray–blue chert cut by veinlets of euhedral pyrite (Fig. 5J). More recently, the Tellus geophysical survey (Young and Donald, 2013) has revealed a laterally extensive magnetic anomaly associated with this unit, with a prominent bulls-eye anomaly over the area of historic exploration (Fig. 6). Diamond drilling down-dip of DDH 91-1 in 2011 intercepted finely laminated (mm-scale) red–brown–black ironstone (sensu stricto) characterized by quartz–hematite–magnetite (DDH 11-BD-01; Fig. 5K; Table 3) (Hollis, 2012). No significant Au grades were intercepted in this drillhole (Hollis, 2012).

3.3. Roof pendants in the late arc-related intrusive suite

In the Craigbardahessiagh granodiorite (464.9 ± 1.5 Ma: Cooper et al., 2008) a roof pendant of dark gray to black, glassy, magnetite-

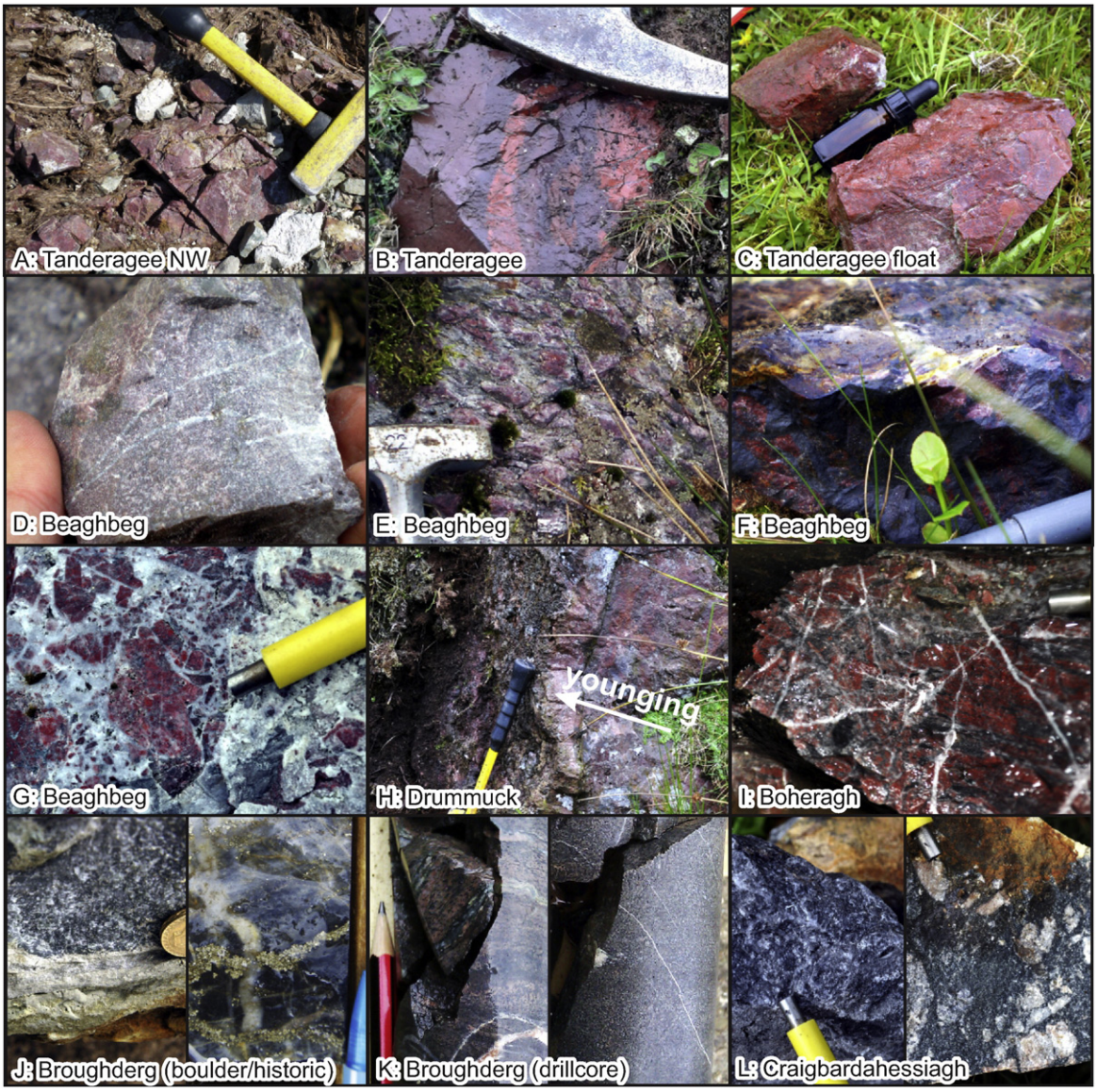

Fig. 5. Representative field photographs of silica-iron-rich rocks from the Tyrone Volcanic Group. (A) Tanderagee NW jasper exposure adjacent to blue–gray chert (location of sample SPH535). (B) Historic Tanderagee outcrop as described by the Geological Survey of Northern Ireland (GSNI) (1979) and Hutton (1983). (C) Jasper float from the Tanderagee area (sample SPH112), northeast of locality b. (D) Pale gray silica-hematite altered tuffaceous rock at Beaghbeg; (E) Silicified and hematite altered tuffs at Beaghbeg. (F) Intensely magnetite brecciated blood-red jasper-like rock at Beaghbeg. (G) Silicification and quartz brecciation at Beaghbeg. (H) Jasper outcropping at Drummuck in the Slieve Gallion Inlier (location of samples MRC627 and MRC628). (I) Boheragh exposure in a thick sequence of graphitic pelite (sample MRC692). (J) Au-rich sulfidic chert float from Broughderg with laminated euhedral pyrite (left — sample MRC690) and a quartz and pyrite veined gray chert intercepted in historic drillhole DDH 91-1 (right). (K) Layered and massive quartz–hematite–magnetite ironstone in drillhole 11-BD-01. (L) Magnetite-rich float at Craigbardahessiagh (left — sample MRC631), which contains small felsic xenoliths (right).

rich chert (Fig. 5L) is poorly exposed for ~50 m (Table 3). It is not clear whether this unit originally formed part of the arc-related Tyrone Volcanic Group or ophiolitic Tyrone Plutonic Group. A reported roof pendant of ironstone in the adjacent ca. 470 Ma Craigballyharky tonalite by Cobbing et al. (1965) was not located.

4. Petrography

Samples of silica-iron-rich rocks from across the Tyrone Igneous Complex were examined in thin section to determine their origin. Although a number were strongly recrystallized, several samples contain relict textures. Significant recrystallization occurs close to the Omagh Thrust (e.g., at Broughderg, Boheragh; Fig. 1C) due to the overthrusting of the Proterozoic Dalradian Supergroup, and the repeated reactivation of the Omagh Thrust since the Ordovician (Cooper et al., 2012). Extensive recrystallization at Bonnety Bush may be due to the reactivation of the Beaghmore Fault associated with SE-directed thrusting.

4.1. Loughmacrory formation

Three samples of jasper float collected from Tanderagee NW, Tanderagee and Creggan Lough (SPH112, SPH113, SPH-CRE), and an outcrop sample from Tanderagee NW (SPH352) (Fig. 4), are the least metamorphosed of all those examined from the Tyrone Igneous Complex. These rocks are dominated by cryptocrystalline to chalcedonic patches and coarse-grained quartz mosaics. Hematite is the dominant iron oxide phase, occurring as translucent, red, fine-grained aggregates. Fine intergrowths of quartz and hematite are

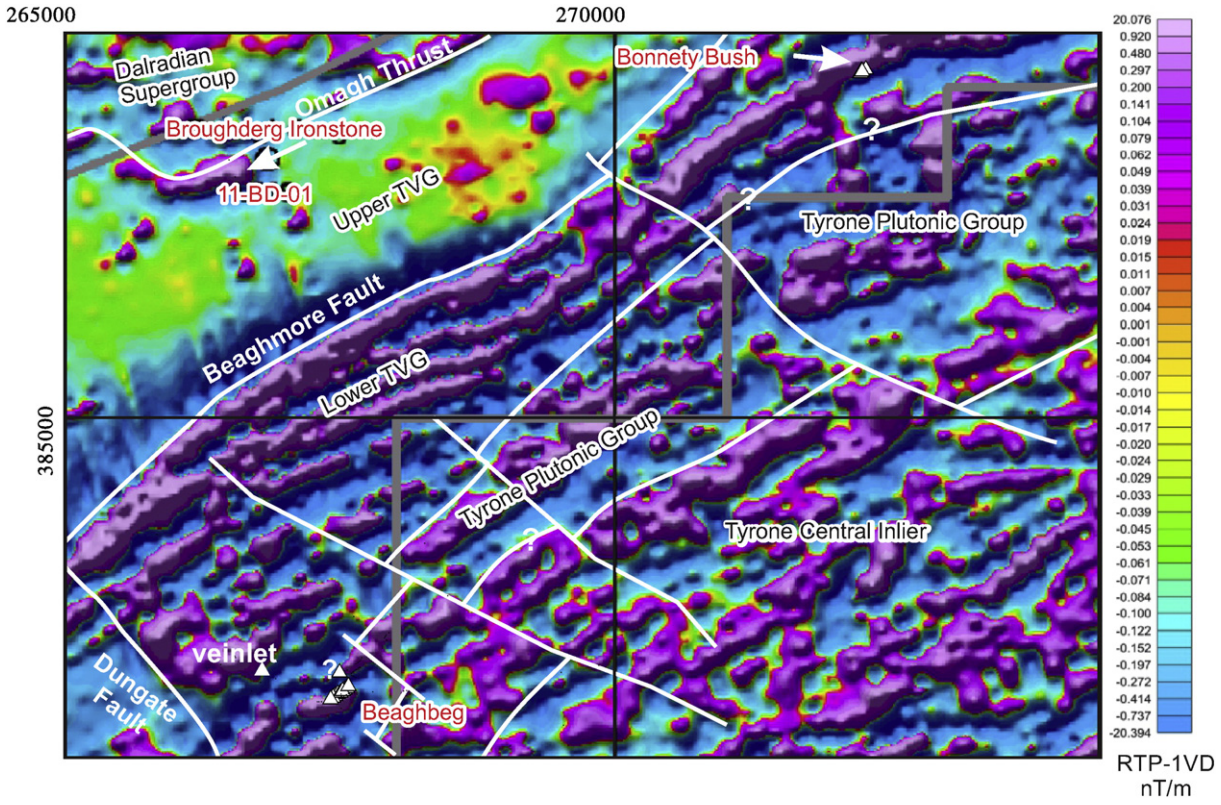

Fig. 6. Interpreted Tellus total magnetic intensity (TMI) map (reduced to pole, 1st vertical derivative — RTP, 1VD) over the Beaghbeg, Bonnety Bush and Broughderg areas of the northeast Tyrone Volcanic Group (TVG).

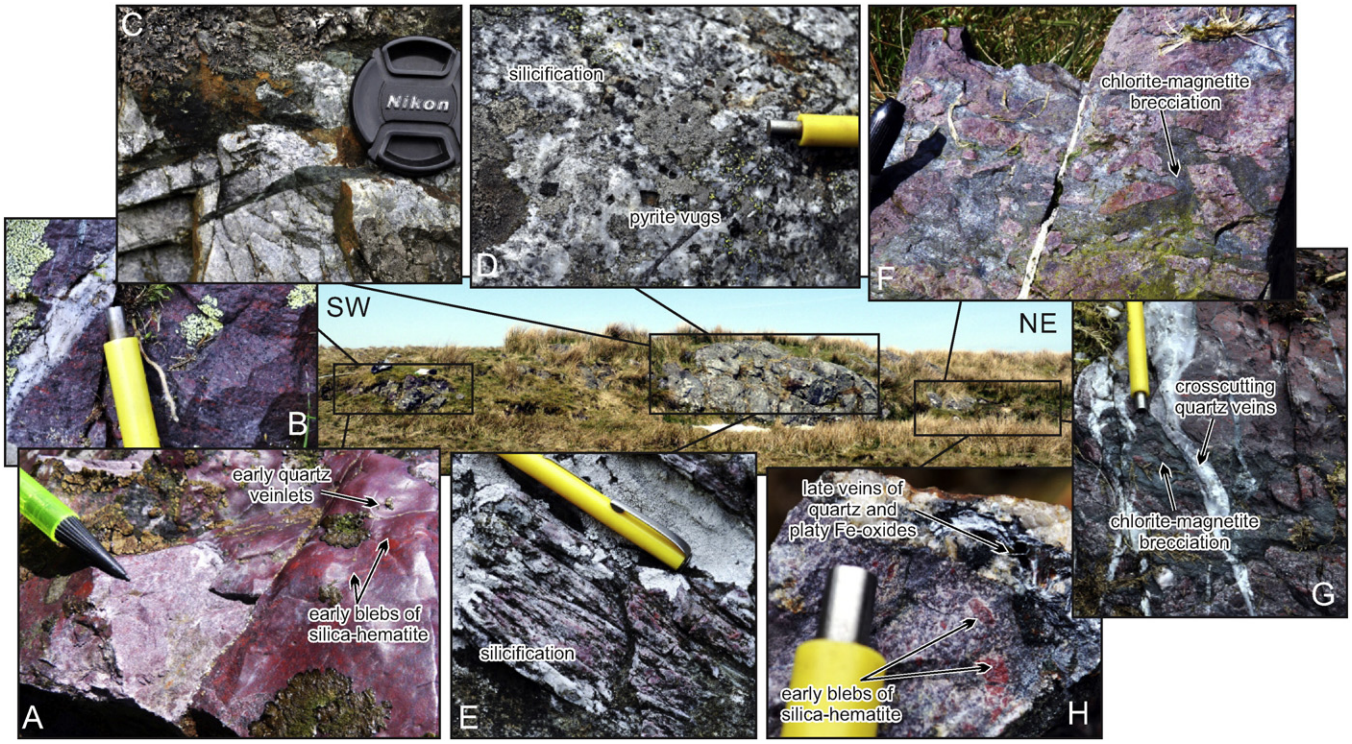

Fig. 7. Field photographs highlighting the range of textures present at Bonnety Bush. (A–B) Early blebs of blood-red quartz–hematite domains are set in a grayer matrix, cut by quartz veinlets. (C–E) Patchy silicification, extensive recystallization and pyrite vugs occur in the central region of the outcrop. (F) Brecciation of quartz-veined and silicified silica-hematite domains by chlorite–magnetite, and a younger generation of quartz veins which cut the chlorite–magnetite matrix (G), some of which contain coarse platy Fe-oxides (H).

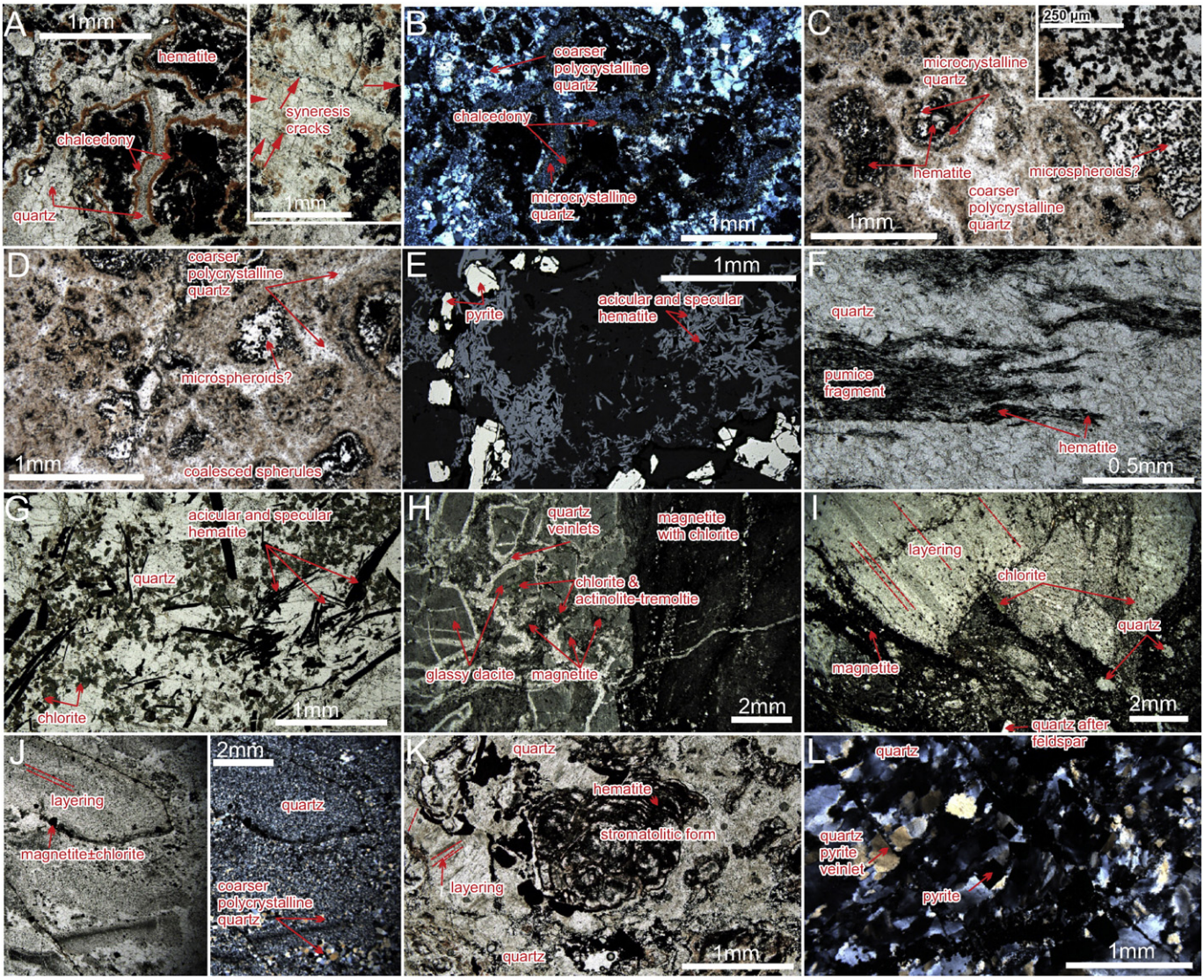

Fig. 8. Representative photomicrographs highlighting the range of textures present. (A) SPH113 Tanderagee jasper float, with quartz-iron oxide spherules in PPL (plane polarized light). (a—inset) Interpreted syneresis cracks. (B) Same image in XPL (cross polarized light). (C–D) SPH351 — Tanderagee NW jasper in PPL, with well preserved coarse quartz-iron oxide and quartz–hematite-rich patches with abundant small (<25 µm wide) Fe-oxide micro-spheroids (left & inset image). (E) SPH-CREG — pyritic jasper float from Creggan Lough in reflected light. (F) SPH10 — Beaghbeg hematite and silica altered tuff in PPL. The margins of the fiamme (pumice fragment) are delineated by very fine hematite. Ovoid vesicles(?) are typically filled with quartz. (G) SPH10 — crosscutting quartz vein in PPL. Hematite occurs in acicular to specular form surrounded by fine-grained scaly masses of chlorite. (H) SPH53 — Beaghbeg, peperitic contact between glassy dacite and magnetite-rich sediment in XPL. (I) SPH182 — Bonnety Bush, contact between a finely laminated silicified and hematite altered siltstone and magnetite-rich unit (possibly a chemical sediment or altered volcanic rock) in PPL. (J) SPH183 — Bonnety Bush silica and hematite altered volcanic breccia in PPL (left) and XPL (right). (K) SPH535 — Tory's Hole (Slieve Gallion) in PPL. The possible incipient stromatolitic form has been highlighted by very fine hematite and surrounded by a fine-grained polycrystalline groundmass of quartz. The fine laminations (red lines) preserved within the coarser grained quartz may be former algal mats. (L) SPH207 — Broughderg recrystallized chert with abundant euhedral pyrite in XPL.

characterized by patches of alternating or broadly concentric zones of chert and iron oxide, surrounded and separated by orange chalcedony (Fig. 8A–D). These features are interpreted to represent coalesced spherules, and are similar in appearance to spherules described from the Mount Windsor Belt, SE Australia (Doyle, 1997), and the Løkken ophiolite, Norway (Grenne and Slack, 2003). Patches of fine coalesced hematite blebs (each <20 µm in diameter; Fig. 8C, D) may be equivalent to the micro-spheroids of Grenne and Slack (2003). In SPH113, fine quartz-iron oxide stringers impart a clastic appearance to the crystalline groundmass between the hematite-rich phases and are likely to represent former syneresis (i.e. subaqueous shrinkage) cracks (Fig. 8A). Minor chlorite is present in all samples. In the Creggan Lough jasper (sample SPH-CREG), abundant acicular red hematite overprints the cores of the spherules (and is spatially associated with subhedral pyrite throughout the rock: Fig. 8E).

A single sample examined from the Tanderagee outcrop (SPH-HUT) is dominated by very fine-grained quartz and hematite. It is classified as either a silica-hematite altered mudstone or intensely altered very fine-grained tuff. Angular patches of polycrystalline quartz ± chlorite throughout the matrix may be replaced crystal fragments incorporated into the sediment. Quartz–chlorite veinlets cut the rock, which locally contain acicular red hematite. Float sample SPH121 from north of Tanderagee (Fig. 4) contains abundant broken sericite-altered feldspar crystal fragments and preserved fiamme, and is classified as a fine grained silica-hematite altered tuff.

4.2. Beaghmore formation

At Beaghbeg and Bonnety Bush, relict textures indicate the original volcanic strata were replaced at or below the seafloor. Sample SPH10 (an intensely altered tuff) from Beaghbeg is dominated by a mineral

assemblage of quartz and hematite, where polycrystalline aggregates of quartz separate red domains of hematite. Recognizable volcaniclastic components include fiamme (Fig. 8F) and polycrystalline quartz that has replaced feldspar. A quartz vein contains acicular to specular forms of hematite and fine-grained scaly masses of chlorite (Fig. 8G), and is cut by late narrow stringers of quartz. In contrast, sample SPH53 contains a peperitic margin between a glassy felsic lava (which resembles blood red jasper in hand specimen) and magnetite-rich sediment. Felsic clasts are aphyric and now composed of a very fine-grained groundmass of recrystallized quartz (with chloritic patches), and display jig-saw fit textures (Fig. 8H), separated by quartz and fine-grained magnetite-rich sediment. A red color is imparted by fine, translucent hematite blebs throughout the quartz. Peperitic contacts signify that the lavas were contemporaneous with the deposition of magnetite-rich chemical sediments. The fine-grained magnetite-rich sediment contains chlorite as coarse irregular forms (possibly representing the complete replacement of rock fragments), sericite, randomly orientated laths of anhydrite, pyrite, and rare chalcopyrite pseudomorphed by covellite.

Most samples from Bonnety Bush are recrystallized and dominated by quartz and iron oxides, with the former commonly occurring as fine-grained polycrystalline aggregates within a microcrystalline quartz groundmass. Tabular forms of medium-grained polycrystalline quartz occur in samples SPH16 and SPH182, and these are likely replacements of feldspar. Iron oxides phases occur in a number of styles at Bonnety Bush. In samples SPH16 and SPH181 (both gray and tuffaceous in appearance) iron oxide phases are predominantly euhedral magnetite, which in the latter sample has been partly pseudomorphed by hematite. In contrast, sample SPH180 (a blood red unit which resembles jasper) is dominated by recrystallized silica-hematite, with only minor euhedral magnetite. A weak foliation throughout SPH180 is defined by patches and discontinuous stringers of hematite throughout a groundmass of aligned quartz. Hematite occurs as aggregates or recrystallized small globules in the matrix of SPH180, with some smaller patches displaying cuspate shapes that are interpreted to be relict glass shards or spherules. In sample SPH17 irregular patches and stringers of mainly hematite occur along with minor goethite and associated euhedral magnetite. Interstitial apatite crystals occur as fine, hexagonal grains within a magnetite-rich layer, and these contain minute inclusions of hematite. Rare blebs of chalcopyrite pseudomorphed by covellite occur as inclusions in some magnetite. Chlorite, tremolite–actinolite and sericite also occur in most samples from Bonnety Bush.

Relationships between silica and iron-rich rocks and surrounding lithologies at Bonnety Bush are best represented in samples SPH182 and SPH183. In sample SPH182, quartz ± hematite domains that resemble jasper in hand specimen are separated by interconnected fine-grained magnetite. Layering is preserved in the quartz–hematite domains (i.e. 'jasper-like fragments'; Fig. 8I), and is defined by alternating very fine-grained quartz mosaics (peppered with hematite) and coarser grained quartz. This layering is due to the intense silicification and hematization of a finely laminated siltstone. The magnetite-rich areas which separate the quartz ± hematite domains (and occur as large blocks in places: Fig. 7F), contains relict volcanic particles and pyroclasts (with patches and stringers of chlorite and minor sericite), and tabular forms of microcrystalline quartz after feldspar (Fig. 8I). In SPH183, a relict coarse clastic texture is preserved where subrounded to tabular clasts (similar in appearance to the siltstone in SPH182) are composed of a very fine-grained mosaic of quartz and in place fine hematite blebs, separated by coarser domains of polycrystalline quartz (Fig. 8J). Minor, very fine-grained acicular tremolite and chlorite occurs in some former clasts, along with subhedral to euhedral magnetite.

Float sample SPH332 from Beaghmore resembles sample SPH180 from Bonnety Bush, though it contains many more cuspate shards and globules of iron oxides. Sample SPH198 (gray sulfidic chert float) from Evishessan Bridge is dominated by recrystallized and strained quartz, finely disseminated coarse euhedral magnetite, and trace pyrite.

4.3. Slieve Gallion Inlier

In sample SPH535 from Tory's Hole a groundmass of fine-grained, polycrystalline quartz mosaics overprints a relict texture interpreted as microbialites, which may include possible incipient stromatolite-like forms (Fig. 8K). These are characterized by fine, contorted, partly domal laminae, delineated by fine hematite. Similar microbialites (stromatolites and oncolites) were noted by Doyle (1997) in petrographically similar ironstones from the Mount Windsor Belt, SE Australia, also preserved as quartz–hematite. Doyle (1997) described the presence of elliptical to spherical oncolites (0.5–1.5 cm diameter), and stromatolites characterized by relatively flat and fine (8–20 μm) internal laminae composed of quartz or hematite. Fine laminations preserved within the coarser-grained quartz mosaics in sample SPH535, between microbialite fragments, may represent former algal mats (Fig. 8K).

4.4. Broughderg formation

All samples examined from the Broughderg formation are strongly recrystallized and no primary textures are preserved. MRC690 (Broughderg pyritic float) now comprises a mosaic of recrystallized and strained quartz, with abundant layered and disseminated euhedral pyrite (Fig. 8L). Sample SPH193 (gray chert from Broughderg) is similar, but is much more quartz-rich and contains trace sulfides. Patchy chlorite occurs in both samples. Sample MRC692 from Boheragh was not examined in thin section, but is also strongly recrystallized due to the proximity of the Omagh Thrust (Fig. 1B).

5. Geochemistry

5.1. Sampling and analytical techniques

Twenty-three samples from representative localities across the Tyrone Igneous Complex were analyzed for whole-rock geochemistry. Sixteen samples (SPH-prefixed) were analyzed at the University of Southampton and seven (MRC-prefixed) samples at the British Geological Survey, Keyworth. For all samples, major element concentrations were analyzed on fused glass beads by X-ray fluorescence (XRF). All powders were dried at ~100 °C before loss on ignition (LOI) measurements and fusion. Fe_2O_{3T} represents total iron expressed as Fe_2O_3.

For SPH-prefixed samples trace element concentrations were determined by XRF on powder-pellets, and rare earth element concentrations (REE; plus Zr, Rb, Ba, Nb, Y, Th, U, Ga) by inductively coupled plasma mass spectrometry (ICP-MS) following an HF/HNO_3 digest (Hollis et al., 2012, 2013a, 2013b). For MRC-prefixed samples, both trace and rare earth element concentrations were determined by ICP-MS. Samples were digested using $HF/HClO_4/HNO_3$, with any residues fused with NaOH before solutions were combined prior to analysis (as in Cooper et al., 2011). Results are presented as Supplementary Material. Accuracy (%RD) and precision (%RSD) were monitored by repeat analysis of several international standards at the University of Southampton (e.g., JG1a granite, JG3 granodiorite, BEN basalt, GXR-1 jasperoid) and can be considered excellent to very good (<7%) after Jenner (1996) for the majority of elements (detailed in Supplementary Material). Sample SPH161 (Loughmacrory basalt) was analyzed at both laboratories and shows a good match between datasets (Supplementary Material).

Data were also compiled from silica-iron-rich chemical sedimentary rocks worldwide for comparison (listed in Appendix A). Europium (Eu/Eu*) and cerium (Ce/Ce*) anomalies are herein defined by $Eu/Eu^* = Eu_{CN}/(Sm_{CN}xGd_{CN})^{0.5}$ and $Ce/Ce^* = 5Ce_{SN}/(4La_{SN} + Sm_{SN})^{0.5}$ (after Toyoda and Masuda, 1991), using chondrite normalization (CN) values from McDonough and Sun (1995) and shale normalization (SN) values from Piper (1974).

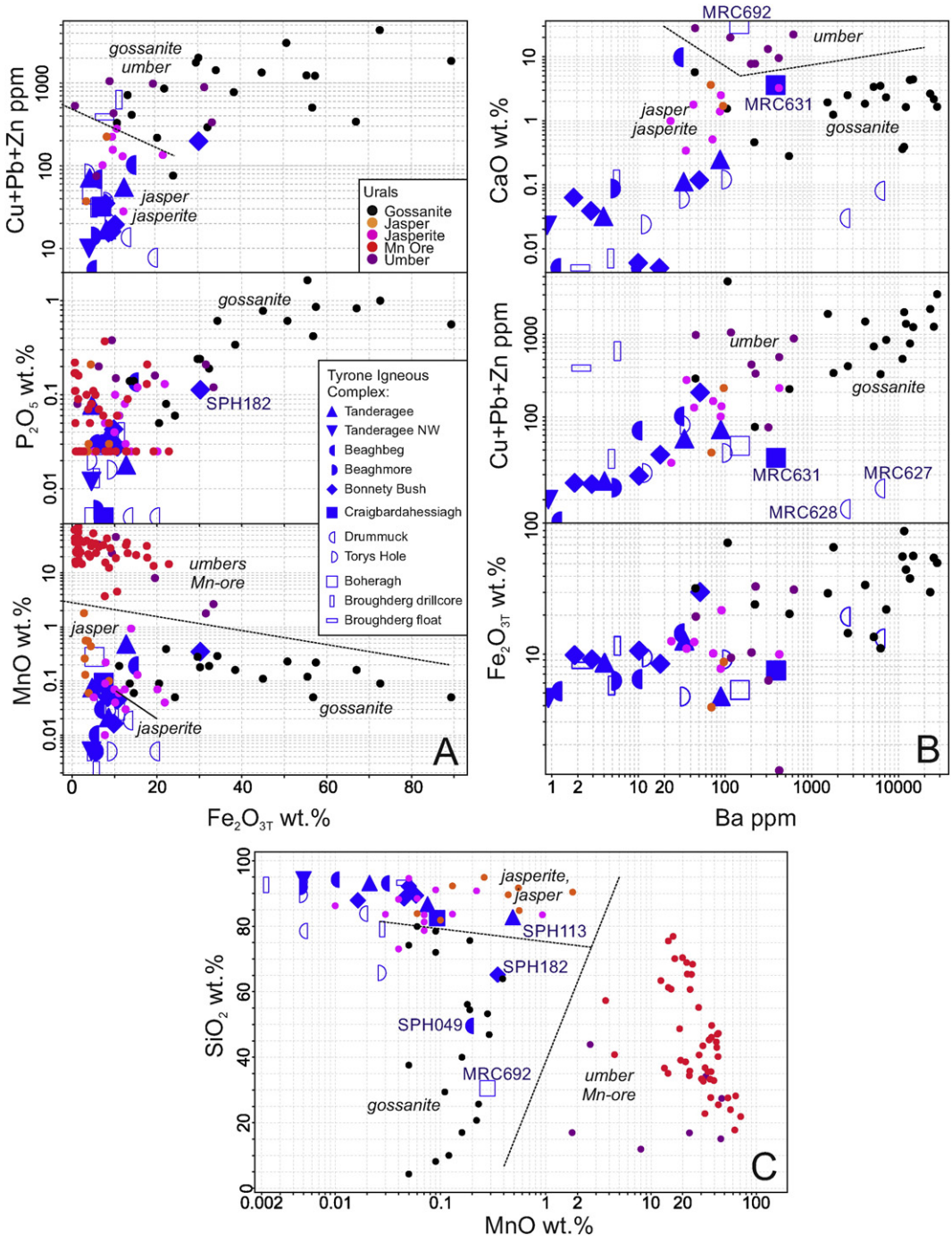

Fig. 9. Bivariate geochemical plots of chemical sedimentary rocks from the Tyrone Igneous Complex and Urals (data from Maslennikov et al., 2012; Brusnitsyn and Zhukov, 2012). (A) Plots of Fe_2O_{3T} vs. MnO, P_2O_5 and Cu + Pb + Zn. Samples from the Tyrone Igneous Complex are most similar to jaspers and jasperites from the Urals, except SPH182 which contains abundant magnetite. (B) Plots of Ba vs. Fe_2O_{3T}, Cu + Pb + Zn and CaO. Samples from Drummuck have similar Ba concentrations to gossanites from the Urals, but significantly lower CaO and base metal concentrations. (C) SiO_2 vs. MnO discrimination plot for jaspers, jasperites, gossanites and umbers from the Urals. Lower SiO_2 concentrations in samples SPH182, SPH049 and MRC692 are due to dilution from higher CaO, Al_2O_3 and/or Fe_2O_{3T}.

Fig. 10. Bivariate and ternary geochemical plots of chemical sedimentary rocks from the Tyrone Igneous Complex and major VMS districts worldwide (data sources listed in Appendix A). (A) Plot of Fe/Ti vs. Al/(Al + Fe + Mn). Samples from the Tyrone Igneous Complex have similar ratios to chemical sedimentary rocks from Bald Mountain, Mount Windsor, Central Arizona, the Iberian Pyrite Belt and Bathurst Mining Camp. Three samples (SPH049, SPH121 and MRC626) have significantly higher Al/(Al + Fe + Mn) values and are comparable to 'tuffites' and similar rocks containing significant detrital components. (B) Eu/Eu* vs. Fe/Ti plot. Few samples from chemical sedimentary rocks worldwide display pronounced positive Eu anomalies like iron formations from the Bathurst Mining Camp. (C) Fe/Ti vs. Al/(Al + Fe + Mn) plot for silica-iron rich rocks from the Urals, Japan and Manus basin. (D) Fe/Ti vs. Cu + Pb + Zn plot. Samples from the Tyrone Igneous Complex are characterized by high Fe/Ti and low Cu + Pb + Zn, like samples from Bald Mountain, Mount Windsor and the Iberian Pyrite Belt. (E) Fe/Ti vs. Al/(Al + Fe + Mn) plot for other volcanic and sedimentary rocks from the Tyrone Igneous Complex (data compiled from Draut et al., 2009; Cooper et al., 2011; Hollis et al., 2012, 2013a, 2013b, 2014). (F) Ternary Th–V–Sc discriminant plot for chemical sedimentary rocks worldwide (left) and rocks from the Tyrone Igneous Complex (right-data sources as in Fig. 10E).

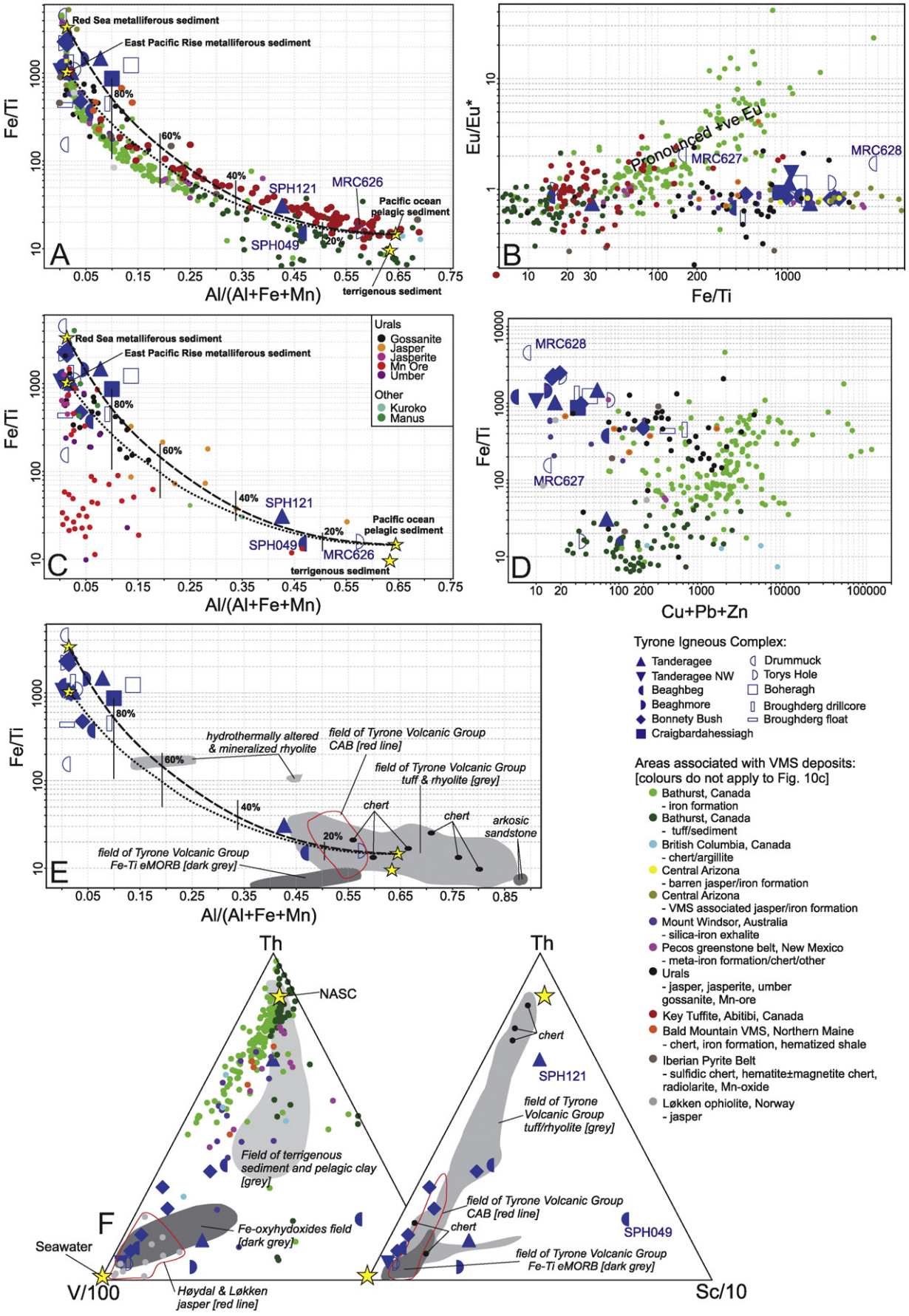
Red Sea metalliferous sediment
East Pacific Rise metalliferous sediment
80%
60%
40%
20%
SPH121
MRC626
SPH049
Pacific ocean pelagic sediment
terrigenous sediment
Fe/Ti
Al/(Al+Fe+Mn)
A
Eu/Eu*
Pronounced +ve Eu
MRC627
MRC628
B
Urals
Gossanite
Jasper
Jasperite
Mn Ore
Umber
Other
Kuroko
Manus
C
D
Cu+Pb+Zn
hydrothermally altered & mineralized rhyolite
field of Tyrone Volcanic Group CAB [red line]
field of Tyrone Volcanic Group tuff & rhyolite [grey]
chert
arkosic sandstone
field of Tyrone Volcanic Group Fe-Ti eMORB [dark grey]
E
Tyrone Igneous Complex:
Tanderagee
Tanderagee NW
Beaghbeg
Beaghmore
Bonnety Bush
Craigbardahessiagh
Drummuck
Torys Hole
Boheragh
Broughderg drillcore
Broughderg float
Areas associated with VMS deposits:
[colours do not apply to Fig. 10c]
Bathurst, Canada - iron formation
Bathurst, Canada - tuff/sediment
British Columbia, Canada - chert/argillite
Central Arizona - barren jasper/iron formation
Central Arizona - VMS associated jasper/iron formation
Mount Windsor, Australia - silica-iron exhalite
Pecos greenstone belt, New Mexico - meta-iron formation/chert/other
Urals - jasper, jasperite, umber gossanite, Mn-ore
Key Tuffite, Abitibi, Canada
Bald Mountain VMS, Northern Maine - chert, iron formation, hematized shale
Iberian Pyrite Belt - sulfidic chert, hematite±magnetite chert, radiolarite, Mn-oxide
Løkken ophiolite, Norway - jasper
Th
NASC
Field of terrigenous sediment and pelagic clay [grey]
Fe-oxyhydoxides field [dark grey]
Seawater
V/100
Høydal & Løkken jasper [red line]
F
chert
SPH121
field of Tyrone Volcanic Group tuff/rhyolite [grey]
field of Tyrone Volcanic Group CAB [red line]
SPH049
field of Tyrone Volcanic Group Fe-Ti eMORB [dark grey]
Sc/10

5.2. Results

Chemical sedimentary rocks from the Tyrone Igneous Complex show significant geochemical variability between localities and within individual units (Figs. 9–12). Jaspers, sulfidic cherts and ironstones are dominated by SiO_2 and Fe_2O_{3T}, have variable Al_2O_3, CaO, MgO concentrations and LOI, plus low TiO_2, MnO, K_2O, Na_2O and P_2O_5 (mean values <0.2 wt.%) (Fig. 9). SiO_2 contents are on average high (mean 82.5 wt.%; max. 94.2 wt.%), but can be as low as 30.5 wt.%, due to higher Fe_2O_{3T}, Al_2O_3 and CaO (which influence the concentrations of other major components due to dilution). Fe_2O_{3T} ranges from 4.6 to 30.2 wt.%, with the highest value in sample SPH182 (Bonnety Bush) that contains abundant magnetite. Sample SPH182 also has high Al_2O_3, MnO, MgO, K_2O and P_2O_5 (Fig. 9).

Al_2O_3 concentrations are low in most samples (<2 wt.%, commonly <0.5 wt.%), although three samples have significantly higher values (4.7–16.4 wt.%). These samples (SPH121, SPH49, MRC626) also had higher concentrations of Rb (4–26 ppm), Th (0.4–2.0 ppm), Zr (26–59 ppm), Sc (5–18 ppm), Nb (0.5–2.4 ppm) and REE_T (24–33 ppm), and high Al/(Fe + Mn + Al) ratios (Fig. 10), indicative of significant detrital components derived from the Tyrone arc (see discussion). Whereas jaspers from the Tanderagee area with well-preserved spherules have low Al_2O_3 (SPH112, SPH113, SPH351: 0.01–1.5 wt.%), the silica and hematite-altered tuff with fiamme and crystal fragments (SPH121) has a much higher Al_2O_3 concentration (4.7 wt.%).

Only three samples contain >0.5 wt.% CaO: MRC631 (3.6 wt.%, Craigbardahessiagh), SPH49 (9.8 wt.%, Beaghbeg) and MRC692 (32.2 wt.%, Boheragh) (Fig. 9). High CaO (32.2 wt.%) and LOI (26.9 wt.%) in MRC692, coupled with low SiO_2, Al_2O_3, Fe_2O_{3T} and S, are indicative of the presence of significant carbonate and graphite components, consistent with its location in a thick sequence of graphitic pelite and quartz-carbonate veining near the Omagh Thrust. Significantly higher Sr in these three samples (Fig. 11) is expected given the high CaO concentrations, as Sr commonly substitutes for Ca in carbonates.

Base metal concentrations are almost universally low, with most samples containing <100 ppm Cu + Pb + Zn (Figs. 10D, 11) and <0.1 wt.% S. The highest base metal and S concentrations are in recrystallized pyrite-bearing cherts at Broughderg. Float sample MRC690 contains 5.8 wt.% S and anomalous levels of Cu (59 ppm), Pb (291 ppm), Zn (277 ppm), As (263 ppm), Ag (2.3 ppm), Mo (24 ppm), Cd (1.4 ppm), Tl (0.2 ppm) and Au (historic assay ~4 g/t). Sample SPH53 from Beaghbeg also has elevated S (0.19 wt.%), but relatively low base-metal concentrations (69 ppm Cu + Pb + Zn) to all other samples analyzed. Higher W occurs at Drummuck (4–8 ppm), Bonnety Bush (9 ppm) and Broughderg (to 7 ppm). Antimony concentrations are extremely variable (0.1–13.5 ppm), and although the dataset is incomplete for this element, high values for MRC-prefixed samples (>6 ppm) are restricted to the Slieve Gallion Inlier (i.e., at Drummuck and Tory's Hole). Jaspers from Drummuck also have significantly higher Ba (2442–6150 ppm: Fig. 9B), Mo (6–7 ppm), positive Eu anomalies (Eu/Eu*) and high Fe + Mn/Al.

The rocks analyzed herein have a wide range of chondrite normalized REE profiles (Fig. 12), reflecting the geochemistry of surrounding strata. All rocks from Tanderagee have moderate to high La/Yb_{CN} ratios (6.0–12.1) regardless of appearance in thin section (Fig. 12A). These ratios are similar to those for host calc-alkaline tuffs and cherts of the Tanderagee Member (Hollis et al., 2012: La/Yb_{CN} 3.8–13.2; Fig. 12A). Samples from Beaghbeg and Beaghmore are flat (La/Yb_{CN} 1.1–3.6), consistent with the intense silica-hematite alteration of surrounding tholeiitic rhyolite breccias and tuffs (Hollis et al., 2012: La/Yb_{CN} 0.9–5.0; Fig. 12B–C), as evident from petrographic analysis. Samples from Bonnety Bush show a range of REE profiles, with SPH16 displaying a flat profile (La/Yb_{CN} 1.8) similar to samples from Beaghbeg (Fig. 12D). Higher REE_T contents at Bonnety Bush are generally positively correlated with increasing Al_2O_3. Samples SPH15, SPH17 and SPH180 have intermediate Al_2O_3 (0.17–2.22 wt.%), REE_T (2.4–3.9 ppm) and high La/Yb_{CN} (6.2–23.4), whereas sample SPH182 (which also displays a steep REE profile: La/Yb_{CN} 7.1) is characterized by significantly higher Al_2O_3 (1.68 wt.%) and REE_T (25.6 ppm). The volcanic sequence at Bonnety Bush includes both island-arc tholeiitic basalt and tuffs with relatively flat REE profiles (La/Yb_{CN} 0.5–2.1) and overlying calc-alkaline tuffs with steep REE profiles (La/Yb_{CN} 6.8–14.7) (Cooper et al., 2011; Hollis et al., 2012; Fig. 12D). REE profiles for samples from Drummuck (La/Yb_{CN} 7.1–9.3) are similar to calc-alkaline lavas and tuffs of the surrounding Whitewater Formation (Hollis et al., 2013b: La/Yb_{CN} 7.9–10.9; Fig. 12F). Samples from Tory's Hole, Craigbardahessiagh and the Broughderg Formation display relatively flat REE profiles, except for sample SPH535 (Fig. 12E, G–H). Modern seawater has a La/Yb_{CN} ratio of ~2.6 (Mitra et al., 1994).

Y/Ho ratios for the majority of samples are comparable to chondritic values (~28; Bau and Dulski, 1999), like all other rocks analyzed from the Tyrone Volcanic Group (see Box and Whisker plots in Fig. 11). Only sample MRC628 from Drummuck has a Y/Ho ratio approaching that of modern seawater (~44 to 74: Bau, 1996; Fig. 11).

Few rocks analyzed herein display positive Eu anomalies (Figs. 10B, 12). The largest positive Eu anomalies (Eu/Eu* 1.4–2.1) were identified in samples from Drummuck and Tanderagee NW (Fig. 12A, F). Minor positive anomalies (Eu/Eu* ~1.1) also occur in samples from Tanderagee (SPH121), Tory's Hole (SPH535) and Boheragh (MRC692) (Fig. 12A, E, H). Most samples analyzed lack pronounced Ce anomalies (either positive or negative: Ce/Ce* ~0.7–1.05). Pronounced negative Ce anomalies occur in samples SPH113 (Tanderagee float with spherules: Ce/Ce* 0.43) and SPH180 (Bonnety Bush: 0.48) (Fig. 12A, D). Positive Ce anomalies occur in samples MRC626 from Tory's Hole (Ce/Ce* 1.14) and SPH332 from Beaghmore (Ce/Ce* 1.44) (Fig. 12C, E).

6. Discussion

6.1. Identification of VMS proximal signatures

The bulk chemical compositions of chemical sedimentary rocks associated with VMS deposits worldwide are dominated by Fe, Si (in chert/quartz and other silicates), Ca (in either carbonates or apatite), and Mn (Peter, 2003). Mg, Al and Ti are generally low unless there is a significant detrital volcanic or volcaniclastic component, whereas S and P are low unless sulfides or apatite are present. Positive inter-element correlations in chemical sedimentary rocks from the Heath Steele Belt (Bathurst Mining Camp) between Fe_2O_3, FeO, Ca, CO_2, P, S, Sr, Ag, As, Au, Bi, Cd, Co, Eu, Ge, Hg, In, Mo, Pb, Sb and Zn were interpreted by Peter and Goodfellow (1996, 2003) to indicate that these elements were genetically related and either co-precipitated from hydrothermal fluids vented on the seafloor, or adsorbed from seawater onto hydrothermal precipitates. In contrast, Si, Ti, Al, K, Mg, Cr, Ga, Hf, Nb, Ni, Sc, Th, U, Y, Zr and the REE (except Eu) were suggested to reflect the presence of detrital aluminosilicates in iron formations of the Bathurst Mining Camp (Peter and Goodfellow, 1996, 2003). The amount of hydrothermal and detrital input is dependent on fluid/rock ratios, bottom current drift, and the degree of basin isolation (Spry et al., 2000). For units that form through replacement processes, element ratios are largely dependent on fluid/rock ratios and precursor compositions.

Major and trace element concentrations for silica-iron-rich rocks from the Tyrone Igneous Complex vary considerably between localities and over short distances (<20 m) along strike. Low Fe/Ti and high Al/(Al + Fe + Mn), Rb, Th, Zr, Sc, Nb and REE_T in samples SPH121 (Tanderagee float), SPH49 (Beaghbeg) and MRC626 (Tory's Hole) indicate these samples contain large amounts of clastic detritus derived from the Tyrone arc or represent silica-hematite-altered volcanic/volcaniclastic rocks. Fe/Ti and Al/(Al + Fe + Mn) ratios for these samples, and chondrite normalized REE profiles (Fig. 12), are similar to calc-alkaline tuffs and rhyolite from across the Tyrone Volcanic Group (Fig. 10E), with analyses plotting away from the seawater end-member on a Th–V–Sc ternary discriminant plot (Fig. 10F). An

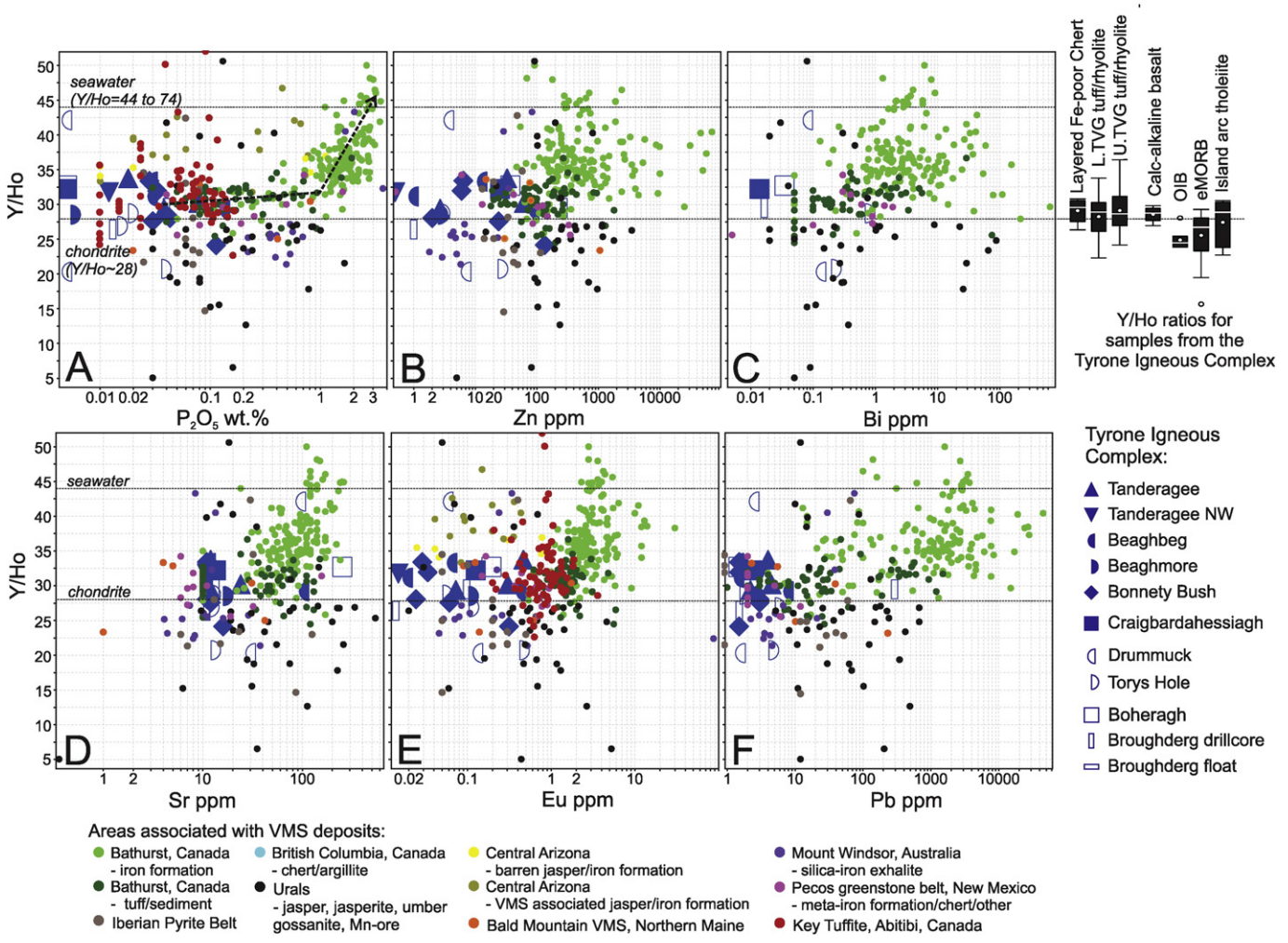

Fig. 11. Bivariate plots of Y/Ho versus selected trace to minor elements of chemical sedimentary rocks from the Tyrone Igneous Complex and major VMS districts worldwide (data sources listed in Appendix A).

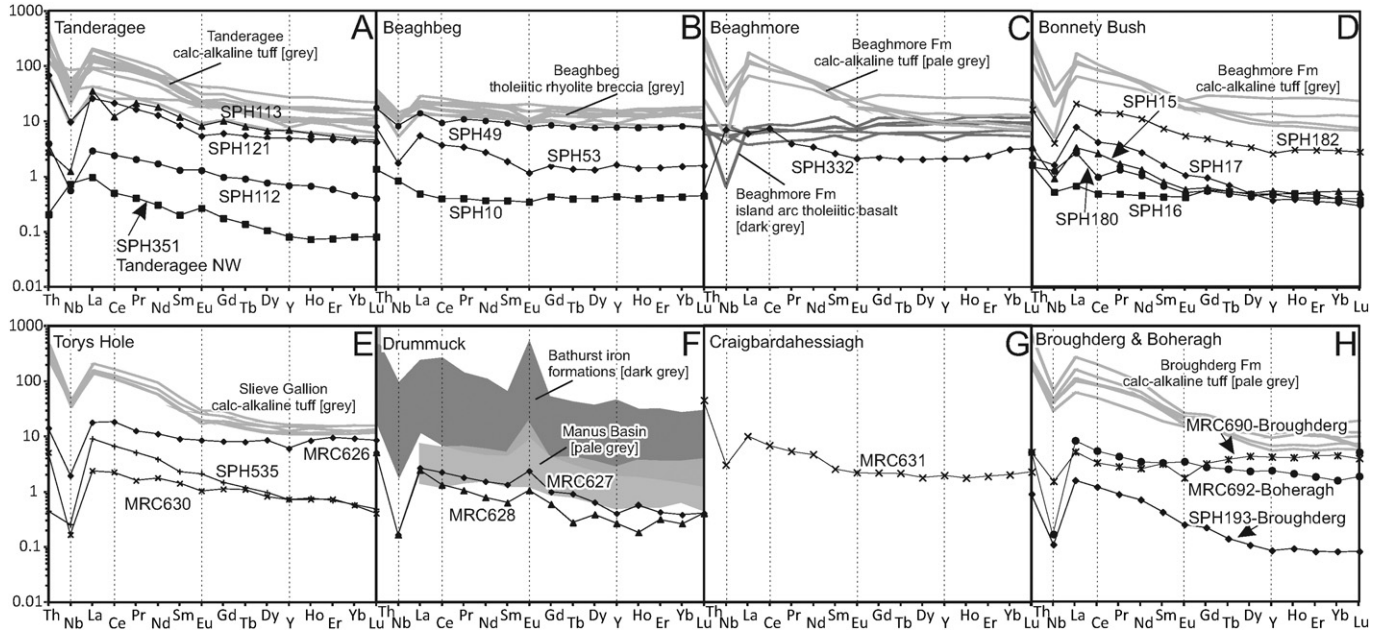

Fig. 12. Chondrite normalized multi-element variation diagrams for chemical sedimentary rocks and surrounding rocks from the Tyrone Igneous Complex (data sources listed in Appendix A). Chondrite normalization values after McDonough and Sun (1995).

abundance of volcanic detritus and the presence of fiamme in SPH121 are consistent with extensive silica-hematite alteration of a fine-grained tuff. Petrographic evidence from Beaghbeg and Bonnety Bush further indicate extensive silica-hematite alteration of tuffs, volcanic breccias (Fig. 8F), glassy flows, and their interaction with magnetite-rich chemical sediments at/under the seafloor (e.g., Fig. 8H). Although the presence of possible microbialites in sample SPH526 (also from Tory's Hole) is hard to reconcile with the replacement of volcanic/volcaniclastic rocks, evidence from Tanderagee, Beaghbeg and Bonnety Bush highlight the range of rock types that can be present and obscured over short distances by intense silica-hematite alteration.

In contrast, other samples from Tanderagee, Tanderagee NW and Creggan Lough, particularly those containing spherules of silica and iron oxides, most likely formed in an environment similar to modern deposits of silica-iron oxyhydroxides (German et al., 1993; Halbach et al., 2002; Hekinian et al., 1993; Juniper and Fouquet, 1988), and jaspers of the Løkken Ophiolite (Grenne and Slack, 2003, 2005) and Mount Windsor Subprovince (Davidson et al., 2001; Doyle, 1997). Such jaspers are interpreted to form by the colloidal fallout from hydrothermal plumes, followed by maturation of gels beneath the seafloor (Grenne and Slack, 2003; see Section 6.3). Chondrite normalized REE profiles similar to host tuffs suggest that the REE chemistry of these rocks is dominated by volcanic detritus, although concentrations are generally low for samples with spherules.

High Ba/Zr, Sb and As in samples from Drummuck are consistent with this unit being the most proximal to mineralization of all those analyzed. A high Y/Ho ratio in sample MRC628 may indicate the presence of a significant seawater component (e.g., Bau, 1996), although the sample lacks a negative Ce anomaly (see following). These findings are also consistent with prospecting results from Drummuck (Section 6.4) and the presence of well-developed positive Eu anomalies (Fig. 12F). Positive Eu anomalies represent a powerful geochemical vector towards potential sites of VMS mineralization (Genna et al., 2014b; Miller et al., 2001; Peter, 2003), having been recognized many modern hydrothermal systems (e.g., Genna et al., 2014b; Michard and Albarède, 1986; Mills and Elderfield, 1995). Under high-temperature (>250 °C), elevated pressures and reducing (low Eh) conditions Eu exists primarily in the 2^+ valence state (Sverjensky, 1984). Venting fluids become reduced through the interaction with rocks in the subsurface at high temperatures (>250 °C), and enriched in Eu due to the preferential breakdown of plagioclase (Douville et al., 1999; Mitra et al., 1994; Sverjensky, 1984), resulting in fluids and precipitates with enrichments in Eu^{2+} and $Eu/Eu^* > 1$. Modern examples include hydrothermal fluids from the Mid Atlantic Ridge (e.g., Snakepit, Lucky Strike), Manus Basin (Fig. 12F), Lau Basin and East Pacific Rise (e.g., Bau and Dulski, 1999; Craddock et al., 2010; Douville et al., 1999). Prominent positive Eu anomalies are also characteristic of VMS proximal chemical sedimentary rocks from the Bathurst Mining Camp (Canada; Peter and Goodfellow, 1996, 2003; Fig. 12F), Løkken ophiolite (Norway; Grenne and Slack, 2005) and Thalanga VMS deposit (Mount Windsor Subprovince; Miller et al., 2001).

The presence of positive Eu anomalies in samples SPH351 (Tanderagee NW outcrop) and SPH112 (float from immediately NE of the original Tanderagee locality; Fig. 4) are consistent with precipitation from hydrothermal fluids that were originally >250 °C and reducing (i.e. associated with the breakdown of plagioclase in underlying strata) at some stage during their formation (see Section 6.3; Sverjensky, 1984). All of these rocks can be classed as silica-iron exhalites (Table 1). While it is also possible that positive Eu anomalies may instead reflect mafic precursor compositions with $Eu/Eu^* > 1$ or the incorporation of detrital feldspar, these samples contain low Al_2O_3, CaO and Na_2O concentrations and no mafic rocks with pronounced positive Eu anomalies have been identified in the Tyrone Igneous Complex (Cooper et al., 2011; Draut et al., 2009; Hollis et al., 2012, 2013b, 2014).

Negative Ce anomalies are characteristic of modern oxic seawater in which Ce^{3+} is oxidized to Ce^{4+} (e.g., Elderfield and Greaves, 1982). As Ce^{4+} is highly insoluble under oxidizing conditions at near to neutral pH it is commonly incorporated into precipitates, adsorbed onto the surfaces of bottom sediments, and precipitated as a colloidal hydroxide (which is subsequently incorporated into Mn nodules and Fe–Mn crusts) (references in Peter, 2003). Consequently, normal oxic seawater is depleted in Ce relative to the other REE, and Mn nodules and crusts are Ce enriched. In the Heath Steele Belt the most negative Ce anomalies are in samples with the greatest amounts of magnetite and/or apatite, reflecting the ability of oxides and phosphates to scavenge REE from Ce depleted seawater (Peter and Goodfellow, 1996, 2003). Pronounced negative Ce anomalies characterize seafloor hydrothermal ironstones deposited in Phanerozoic oceans; such signatures have been identified at the TAG and Rainbow vent fields of the Mid Atlantic Ridge, on the East Pacific Rise, and in numerous VMS-proximal chemical sediments of various age (e.g., Barrett et al., 1988; Slack et al., 2007). There appears to be no systematic relationship between pathfinder element concentrations and the magnitude of Ce anomalies in samples from the Tyrone Igneous Complex. Samples that display negative Ce anomalies include those from Bonnety Bush (SPH180) and Tanderagee (SPH113) (Fig. 12A, C), indicating these rocks have interacted with (or precipitated from) oxidizing seawater. As neither of samples MRC626 (Tory's Hole) and SPH332 (Beaghmore) contain significant amounts of apatite or magnetite the origin for the positive Ce anomalies remains unclear.

6.2. Comparison to VMS associated and barren units worldwide

Comparison between the rocks analyzed here and chemical sedimentary units worldwide (Figs. 9–12) further highlights the VMS prospectivity of the Tyrone Igneous Complex (after Clifford et al., 1992; Peatfield, 2003; Hollis et al., 2014). In their recent review of silica-iron and manganese-rich rocks of the Urals, Maslennikov et al. (2012) suggested that jaspers, jasperites, umbers and gossanites (described in Table 1) may be distinguished geochemically from each other. The data presented by Maslennikov et al. (2012) are plotted here in Fig. 9, with most samples of the Tyrone Igneous Complex resembling jaspers and jasperites (see Table 1 for distinguishing characteristics). Such rocks are characterized by low Fe_2O_3, Cu, Pb, Zn, P_2O_5 and MnO, and high SiO_2 contents. This is consistent with the petrographic work presented here, that indicates silica-iron-rich rocks from the Tyrone Igneous Complex are jaspers/silica-iron exhalites with varying amounts of volcanic detritus (at Tanderagee NW, Creggan Lough and Tory's Hole, Drummuck) or intensely silica-hematite altered lavas and tuffs (at Tanderagee, Beaghbeg and Bonnety Bush). Sample SPH182 (Bonnety Bush) contains higher Cu + Pb + Zn and high Fe_2O_3 similar to gossanites and umbers of the Urals (Fig. 9A). The high Fe in this sample is due to the magnetite and chlorite that have brecciated the SE-end of the Bonnety Bush outcrops (Fig. 7F). High Ba contents in jaspers from Drummuck are comparable to Urals gossanites, although the latter have significantly higher Cu + Pb + Zn, CaO, P_2O_5 and Fe_2O_3. In contrast, sulfidic cherts from Broughderg have high Cu + Pb + Zn, but low Ba contents (Fig. 9A–B). Chondrite normalized REE profiles from the lower Tyrone Volcanic Group are comparable to jaspers, jasperites and gossanites from the Urals; however, REE profiles are more dependent on incorporated/replaced volcanic components than the composition of the hydrothermal fluid (Peter and Goodfellow, 1996, 2003).

The geochemistry of silica-iron-rich chemical sedimentary rocks from other major VMS camps worldwide are shown in Figs. 10–12. Although samples from the Tyrone Igneous Complex have comparable Fe/Ti and Al/(Fe + Mn + Al) ratios to iron formations of the Bathurst Mining Camp, the latter are characterized by significantly higher base metal concentrations (Fig. 10D), Th (Fig. 10F), P_2O_5 and more pronounced positive Eu anomalies (Fig. 10B). Clear correlations are also apparent between Y/Ho and a number of trace elements in the Bathurst iron formations (Fig. 11). Y/Ho ratios (towards a ratio typical of seawater) are positively correlated with (significantly higher) P_2O_5, Sr, Zn, Pb, Bi, Eu and Fe/Ti. No such trends are apparent for the samples analyzed from Northern Ireland, or in chemical sedimentary rocks from the

Pecos greenstone belt, Central Arizona, Mount Windsor Subprovince, Iberian Pyrite Belt and Urals (Fig. 11). Only sample MRC628 from Drummuck has a Y/Ho ratio approaching seawater. It is important to note here that the Bathurst iron formations represent the distal expressions of VMS deposits. VMS-proximal, laterally-restricted jaspers and exhalites of the Iberian Pyrite Belt and Mount Windsor Subprovince are more comparable to samples from the Tyrone Igneous Complex.

Tuffaceous exhalites from the Kuroko district and Abitibi greenstone belt have significantly lower Fe/Ti and higher Al/(Fe + Mn + Al) ratios than most samples analyzed here (Fig. 10A, C). This is consistent with the presence of significant detrital components in these rocks (e.g., Kalogeropoulos and Scott, 1983, 1989) or their formation through the replacement of volcanic rocks (e.g., Genna et al., 2014a; Liaghat and MacLean, 1992). Samples SPH121 (Tanderagee float), SPH49 (Beaghbeg) and MRC626 (Tory's Hole) from the Tyrone Igneous Complex are comparable to these rocks. In summary, silica-iron-rich rocks from Northern Ireland are most similar to silica-iron exhalites of the Mount Windsor Subprovince, SE Australia (Figs. 10A, 11); jaspers from the Løkken Ophiolite, Norway (Fig. 10F); Central Arizona; Bald Mountain (Northern Maine), Iberian Pyrite Belt, and jaspers and japerites of the Urals.

6.3. Genesis of silica-iron-rich rocks in the Tyrone Igneous Complex

Evidence presented here indicates that the silica-iron-rich rocks (or ironstones — sensu lato) of the Tyrone Igneous Complex formed by a variety of processes. The presence of spherules (at Tanderagee NW, Creggan Lough, and in float from Tanderagee) and possible microbialites (at Tory's Hole) indicate at least some of these rocks formed by the precipitation from hydrothermal fluids vented onto the seafloor (e.g., Davidson et al., 2001; Grenne and Slack, 2003, 2005). Furthermore, the incorporation of jasper pebbles into overlying strata at Tanderagee (Hutton, 1983) suggests that the lithification of the primary silica-iron oxyhydroxide gel to coherent jasper was relatively rapid. As silica-iron deposits form by low temperature (<100 °C) precipitation of Si–Fe oxyhydroxides from diffuse vent sites (references in Grenne and Slack, 2003), the pronounced positive Eu anomalies at Tanderagee NW and Drummuck may have been imparted from more evolved fluids as the hydrothermal system developed (e.g., Davidson et al., 2001). Minerals precipitated from these hotter fluids will carry excess Eu in solution. These hotter fluids would have carried Eu^{2+}, and any minerals with appropriate residence sites for Eu would bear a similar positive Eu anomaly. Such fluids may have precipitated late quartz–chlorite ± magnetite veins (which are clearly fracture controlled, post-lithification of the Si–Fe gels) and/or introduced pathfinder elements associated with VMS mineralization (e.g., Cu, Pb, Zn, Au, Ag, As, Sb, Sn, Tl). In the Mount Windsor Subprovince, hotter fluids with higher H_2S introduced Si–Cu–Pb–Zn–Se–Tl ± Eu to the system, precipitated disseminated pyrite and magnetite through the jasper lens, and altered fluid pathways to chlorite-carbonate (Davidson et al., 2001). Similarly, at Drummuck (and possibly Tanderagee NW), silicification and mineralization (Zn–Pb–Cu–Au–Ag) would have formed in the shallow subsurface in porous and permeable tuffaceous strata (see Section 6.4). Syneresis cracks and chalcedony in jaspers at Tanderagee NW (Fig. 8A) most likely formed during diagenesis (e.g., Grenne and Slack, 2003).

In contrast to most samples from the Loughmacrory Formation and Slieve Gallion Inlier, samples from Beaghbeg and Bonnety Bush indicate that these silica-iron-rich rocks formed predominantly through the replacement of tuffaceous rocks, volcanic breccias and originally glassy felsic rocks at/below the seafloor. The presence of sericite, anhydrite, pyrite, and rare chalcopyrite (pseudomorphed by covellite) in the magnetite-rich sediment at Beaghbeg may indicate that hotter systems (>100 °C) were also active at this time (albeit relatively distal to Beaghbeg). The peperitic contacts between glassy lavas and magnetite-rich chemical sediment, suggest these rocks were replaced at, or just below, the seafloor in permeable strata. As clasts of silica-hematite altered volcanic/volcaniclastic rocks also occur in overlying rocks at Beaghbeg, these rocks either formed rapidly or were exposed by faulting shortly after formation. Extensive chlorite–magnetite brecciation of earlier silica-hematite altered lithologies at Bonnety Bush (Fig. 7F) may have occurred during the venting of hotter fluids that locally introduced some pathfinder elements (e.g., Cu, Zn, Sb) as described above. Subsequent quartz veining (Fig. 7G–H) occurred either as the system waned or much later.

The extensive recrystallization of silica-iron-rich rocks at Broughderg and Boheragh has obliterated primary textures and obscured determination of their origin, although the relatively flat REE profiles indicate that these rocks have received little volcanic detritus (except sample SPH193) and most likely precipitated from seawater. The abundance of sulfides and pathfinder elements at Broughderg may indicate the presence of a local hydrothermal upflow zone nearby, consistent with the intense chloritization of surrounding strata (Hollis, 2012). Fe-poor, bedded gray chert crops out at a similar stratigraphic level to the Broughderg ironstone approximately 1 km along strike.

6.4. Implications for regional exploration

This study explores the use of bulk ironstone geochemistry (sensu lato) as an inexpensive tool for regional VMS exploration. Key areas identified here that warrant further investigation include Drummuck, Tanderagee NW-Creggan Lough, Bonnety Bush and Broughderg. Systematic sampling of these units along strike is recommended to identify the most intense hydrothermal signatures and potentially locate mineralization. Although exposure in many of these areas is poor, due to extensive glacial deposits, regional Tellus airborne geophysics (Young and Donald, 2013) and historic ground-based geophysics are both able to delineate silica-iron-rich rocks along strike. The Broughderg ironstone corresponds with a Tellus total magnetic intensity (TMI) high which continues for at least 5 km to the SW as revealed by tilt and first vertical derivative (1VD) responses (Young and Donald, 2013). The overlying sequence of graphitic pelite is apparent on Tellus electromagnetic (EM) apparent conductivity and Ennex induced polarization (IP) chargeability maps. Drilling down dip of historic drillhole 91–1 at Broughderg in 2011 intersected only low (at or near lower limits of detection) contents of pathfinder elements (Au, Ag, Cu, Pb, Hg, Mo, Te, Tl) and anomalous levels of As (to 11 ppm), Sb (to 6 ppm) and Zn (to 88 ppm) (Hollis, 2012). This suggests this drillhole is located further away from a major hydrothermal fluid upflow zone than the original Ennex holes and bedrock source of the float samples. High concentrations of Ag, As, Au, Cd, Cu, Mo, Pb, S, Tl and Zn in samples analyzed herein suggest this unit warrants further attention.

Exposure around Bonnety Bush is among the poorest in the Tyrone Igneous Complex. The nearest outcrops of this volcanic sequence along strike are ~7 km to the SW (at Broughderg River, near Evishessan Bridge) and 3 km to the NE (near Boley) (Fig. 1C). In addition to the whole rock geochemical data presented here, the potential for mineralization in this area is highlighted by historic prospecting results and deep overburden Pionjar sampling. Historic Ennex samples of jasper float (with stringer pyrite) and mineralized tuff assay up to 4.54 g/t Au and 2.98% Zn respectively. Deep overburden samples contain up to 77 ppb Au, 750 ppm Pb, 960 ppm Zn and 365 ppm Cu at Bonnety Bush. Systematic short drilling along strike would be warranted due to the presence of thick glacial deposits and peat across the area. Underlying rocks exposed to the SE include intensely silica-epidote altered tholeiitic basalt, with demagnetized zones evident from Tellus TMI maps. Recognition that the thick and laterally extensive ironstone unit outcropping at Bonnety Bush is predominantly replacive in origin is indicative of significant hydrothermal activity occurring at the time. Identification of higher temperature hydrothermal upflow zones within this area is a key priority.

Little exploration for VMS mineralization has been done in the Slieve Gallion Inlier. Historic prospecting downstream of the Drummuck ironstone has identified barite cobbles and silicified tuffs with 0.23% Zn, 0.11% Pb and 0.5 ppm Ag. Abundant mineralized float also occurs ~900 m to the northeast (to 3% Zn, 0.23% Pb, 0.15% Cu and 23 ppm Ag) in an adjacent stream section. The Drummuck ironstone corresponds with a Tellus TMI-tilt and 1VD anomaly which extends for ~400 m along strike before it is cut off at each end by NW–SE trending faults (Hollis et al., 2013b). This area is a key target for exploration, with Tellus soil and stream sediment Sb anomalies immediately downstream, and areas of high Au in stream sediments to the east (Hollis et al., in press). Zinc and Pb stream sediment anomalies also occur ~1.5 km to the northeast associated with ironstone float at a similar stratigraphic level in the Whitewater Formation where quartz-sericite-pyrite-fuchsite altered tuffs crop out (Hollis et al., in press).

Although silica-iron-rich float is abundant throughout the Loughmacrory Formation (Fig. 1C), there is little known mineralization in the vicinity (either from outcrop or float). Low level Au mineralization is associated with stringer pyrite at Creggan Lough (0.7 g/t from grab sample SPH-CRE), although pathfinder concentrations are low (e.g., 4 ppm As, 0.26 ppm Sb, 14 ppm Cu, 2 ppm Zn). Higher assay values (to 3 g/t Au) have been obtained from jasper float ~1 km NE of the Creggan Lough outcrops. Due to extensive farming throughout the Tanderagee, Tanderagee NW, Creggan Lough and Loughmacrory areas, jasper float is abundant, often as small fragments in freshly plowed fields. Systematic sampling of float across the region may prove fruitful. Our geochemical data suggest that the Tanderagee NW and possibly Creggan Lough areas are prospective for VMS mineralization. Although float sample SPH112 (with well-developed spherules and a positive Eu anomaly) may originate from the jasper outcrop at Tanderagee NW, abundant small float clasts similar to SPH112 were noted in several fields immediately to the NE of the Tanderagee outcrop (Fig. 4). These clasts parallel a series of EM anomalies and may suggest the Tanderagee 'ironstone' is more prospective to the NE.

Low concentrations of pathfinder elements at Beaghbeg, Tory's Hole and Boheragh indicate these areas are the least prospective for VMS mineralization of all those sampled. This is consistent with the lack of mineralized float in these areas.

7. Conclusions

This work has further highlighted both the VMS prospectivity of the Tyrone Igneous Complex and use of 'ironstone' bulk geochemical data for regional mineral exploration. Silica-iron-rich rocks formed from hydrothermal fluids venting onto the seafloor at Tanderagee NW, Creggan Lough, Tory's Hole and Drummuck, and by the replacement of tuffaceous rocks and glassy lavas at/below the seafloor at Beaghbeg, Bonnety Bush and Tanderagee. Rocks of the uppermost Tyrone Volcanic Group are strongly recrystallized jaspers and sulfidic cherts. Whole rock geochemical characteristics are similar to silica-iron exhalites of the Mount Windsor Subprovince (SE Australia), and jaspers of Central Arizona, Bald Mountain (Northern Maine), the Urals, Iberian Pyrite Belt, and Løkken ophiolite (Norway). Several key areas are identified herein that are prospective for VMS mineralization; these include Drummuck, Bonnety Bush, Tanderagee NW-Creggan Lough and Broughderg. Samples with positive Eu anomalies, elevated Cu + Pb + Zn, Au, Fe/Ti, Fe/Mn, Sb, Ba/Zr and Fe + Mn/Al (together with low REE_{Total}, Sc, Zr and Th) have a greater hydrothermal component and are potentially more VMS-proximal.

Acknowledgments

The authors thank Andy Milton and Matthew Cooper for ICP-MS analysis and Ian Croudace for XRF analysis at the University of Southampton. Robin Taggart, Hilary Clarke, Gavin Berkenheger, Raymond Keenan and Dalradian Gold personnel are thanked for many insightful field discussions. SPH gratefully acknowledges PhD funding from the British Geological Survey (BGS University Funding Initiative), Dalradian Gold Ltd, Geological Survey of Northern Ireland, University of Southampton, Metallum Resources and Natural History Museum, London. Geochemical analysis of MRC-prefixed samples was funded by the Department of Enterprise, Trade and Investment, Northern Ireland. MRC publishes with permission of the Executive Director of the BGS (NERC). CSIRO reviewers Joanna Parr and Walid Salama are thanked for many constructive comments on an earlier edition of this manuscript. Editor Robert Ayuso, reviewer Jan Peter and an anonymous reviewer greatly improved this paper.

Appendix A

List of geochemical data sources included herein.

Bald Mountain, Northern Maine (Slack et al., 2003); Bathurst Mining Camp, Canada (Peter and Goodfellow, 1996, 2003); Myra Falls, British Columbia (Jones et al., 2006); Central Arizona (Slack et al., 2007), Iberian Pyrite Belt (Leistel et al., 1998); Kuroko deposits, Japan (Kalogeropoulos and Scott, 1989); Løkken ophiolite, Norway (Grenne and Slack, 2005); Manus basin (Binns, 2006); Millenbach area, Abitibi (Kalogeropoulos and Scott, 1989); Mount Windsor Subprovince, SE Australia (Davidson et al., 2001); Pecos greenstone belt (Slack et al., 2009); Tyrone Igneous Complex (Cooper et al., 2011; Draut et al., 2009; Hollis et al., 2012, 2013b, 2014); Urals (Brusnitsyn and Zhukov, 2012; Maslennikov et al., 2012).

Appendix B. Supplementary data

Supplementary data to this article can be found online at http://dx.doi.org/10.1016/j.gexplo.2015.09.001.

References

Allaby, M. (Ed.), 2013. Oxford Dictionary of Geology & Earth Sciences. Oxford University Press, New York (660 pp.).

Alsop, G.I., Hutton, D.H.W., 1993. Major southeast-directed Caledonian thrusting and folding in the Dalradian rocks of mid-Ulster: implications for Caledonian tectonics and mid-crustal shear zones. Geol. Mag. 130, 233–244.

Barrett, T.J., Jarvis, I., Longstaffe, F.J., Farquhar, R., 1988. Geochemical aspects of hydrothermal sediments in the eastern Pacific Ocean: an update. Can. Mineral. 26, 841–858.

Barrett, T.J., MacLean, W.H., Tennant, S.C., 2001. Volcanic sequence and alteration at the Parys Mountain volcanic-hosted massive sulfide deposit, Wales, United Kingdom: applications of immobile element lithogeochemistry. Econ. Geol. 96, 1279–1305.

Bau, M., 1996. Controls on the fractionation of isovalent trace elements in magmatic and aqueous systems: evidence from Y/Ho, Zr/Hf, and lanthanide tetrad effect. Contrib. Mineral. Petrol. 123, 323–333.

Bau, M., Dulski, P., 1999. Comparing yttrium and rare earths in hydrothermal fluids from the Mid-Atlantic Ridge: implications for Y and REE behaviour during near-vent mixing and for the Y/Ho ratio of Proterozoic seawater. Chem. Geol. 155, 77–90.

Bekker, A., Slack, J.F., Planavsky, N., Krapež, B., Hofmann, A., Konhauser, K.O., Rouxel, O.J., 2010. Iron formation: the sedimentary product of a complex interplay among mantle, tectonic, oceanic, and biospheric processes. Econ. Geol. 105, 467–508.

Binns, R.A., 2006. Data report: petrography and geochemistry of jasperoids from site 1189, ocean drilling program Leg 193. In: Barriga, F.J.A.S., Binns, R.A., Miller, D.J., Herzig, P.M. (Eds.), Proceedings of the Ocean Drilling ProgramScientific Results vol. 193. Ocean Drilling Program, College Station, TX, pp. 1–30. http://dx.doi.org/10.2973/odp.proc.sr.193.211.2006.

Brusnitsyn, A.I., Zhukov, I.G., 2012. Manganese deposits of the Devonian Magnitogorsk palaeovolcanic belt (Southern Urals, Russia). Ore Geol. Rev. 47, 42–58.

Carvalho, D., Barriga, F.J.A.S., Munha, J., 1999. Bimodal-siliciclastic systems — the case of the Iberian Pyrite Belt. In: Barrie, C.T., Hannington, M.D. (Eds.), Volcanic-Associated Massive Sulfide Deposits: Processes and Examples in Modern and Ancient Settings. Reviews in Economic Geology 8, pp. 375–402.

Chew, D.M., Flowerdew, M.J., Page, L.M., Crowley, Q.G., Daly, J.S., Cooper, M.R., Whitehouse, M.J., 2008. The tectonothermal evolution and provenance of the Tyrone Central Inlier, Ireland: Grampian imbrication of an outboard Laurentian microcontinent? J. Geol. Soc. Lond. 165, 675–685.

Clifford, J.A., Earls, G., Meldrum, A.H., Moore, N., 1992. Gold in the Sperrin Mountains, Northern Ireland: an exploration case history. In: Bowden, A.A., Earls, G., O'Connor, P.G., Pyne, J.F. (Eds.), The Irish Minerals Industry 1980–1990. Irish Association for Economic Geology, Dublin, pp. 77–87.

Cobbing, E.J., Manning, P.I., Griffith, A.E., 1965. Ordovician–Dalradian unconformity in Tyrone. Nature 206, 1132–1135.

Colman, T.B., Cooper, D.C., 2000. 2nd Edition. Exploration for Metalliferous and Related Minerals in Britain: A guide 1. British Geological Survey,/DTI Minerals Programme Publication (78 pp.).
Cooper, M.R., Mitchell, W.I., 2004. Midland Valley Terrane. In: Mitchell, W.I. (Ed.), The Geology of Northern Ireland. Our Natural Foundation, 2nd edn Geological Survey of Northern Ireland, pp. 25–40.
Cooper, M.R., Crowley, Q.G., Rushton, A.W.A., 2008. New age constraints for the Ordovician Tyrone Volcanic Group, Northern Ireland. J. Geol. Soc. Lond. 165, 333–339.
Cooper, M.R., Crowley, Q.G., Hollis, S.P., Noble, S.R., Roberts, S., Chew, D., Earls, G., Herrington, R., Merriman, R.J., 2011. Age constraints and geochemistry of the Ordovician Tyrone Igneous Complex, Northern Ireland: implications for the Grampian orogeny. J. Geol. Soc. Lond. 168, 837–850.
Cooper, M.R., Anderson, H., Walsh, J.J., Van Dam, C.L., Young, M.E., Earls, G., Walker, A., 2012. Palaeogene Alpine tectonics and Icelandic plume-related magmatism and deformation in Northern Ireland. J. Geol. Soc. Lond. 169, 29–36.
Craddock, P.R., Bach, W., Seewald, J.S., Rouxel, O.J., Reeves, E., Tivey, M.K., 2010. Rare earth element abundances in hydrothermal fluids from the Manus basin, Papua New Guinea: indicators of sub-seafloor hydrothermal processes in back-arc basins. Geochim. Cosmochim. Acta 74, 5494–5513.
Davidson, G.J., Stolz, A.J., Eggins, S.M., 2001. Geochemical anatomy of silica iron exhalites: evidence for hydrothermal oxyanion cycling in response to vent fluid redox and thermal evolution (Mt. Windsor Subprovince, Australia). Econ. Geol. 96, 1201–1226.
Douville, E., Bienvenu, P., Charlou, J.L., Donval, J.P., Fouquet, Y., Appriou, P., Gamo, T., 1999. Yttrium and rare earth elements in fluids from various deep-sea hydrothermal systems. Geochim. Cosmochim. Acta 63, 627–643.
Doyle, M.G., 1997. A Cambro–Ordovician submarine volcanic succession hosting massive sulfide mineralisation: Mount Windsor Subprovince, Queensland. Unpublished PhD thesis, University of Tasmania, Australia.
Draut, A.E., Clift, P.D., Amato, J.M., Blusztajn, J., Schouten, H., 2009. Arc–continent collision and the formation of continental crust: a new geochemical and isotopic record from the Ordovician Tyrone Igneous Complex, Ireland. J. Geol. Soc. Lond. 166, 485–500.
Dunning, G.R., Krogh, T.E., 1985. Geochronology of ophiolites in the Newfoundland Appalachians. Can. J. Earth Sci. 22, 1659–1670.
Elderfield, H., Greaves, M.J., 1982. The rare earth elements in seawater. Nature 296, 214–218.
Ennex International plc, 1987. Report on exploration activities during 1987 in UM1-4/81, UM5/84, FG1/85 (Counties Tyrone and Londonderry), and in UM6-7/84 (County Antrim). Unpublished report submitted to GSNI by Ennex International plc.
Galley, A.G., Hannington, M.D., Jonasson, I.R., 2007. Volcanogenic massive sulphide deposits. In: Goodfellow, W.D. (Ed.), Mineral Deposits of Canada: A Synthesis of Major Deposit-Types, District Metallogeny, the Evolution of Geological Provinces, and Exploration Methods. Geological Association of Canada, Mineral Deposits Division, Special Publication 5, pp. 141–161.
Genna, D., Gaboury, D., Roy, G., 2014a. The Key Tuffite, Matagami Camp, Abitibi Greenstone Belt, Canada: petrogenesis and implications for VMS formation and exploration. Mineral. Deposita 49, 489–512.
Genna, D., Gaboury, D., Roy, G., 2014b. Evolution of a volcanogenic hydrothermal system recorded by the behaviour of LREE and Eu: case study of the Key Tuffite at Bracemac-McLeod deposits, Matagami, Canada. Ore Geol. Rev. 63 (160), 177.
Geological Survey of Northern Ireland (GSNI), 1979. Pomeroy, Northern Ireland Sheet 34. Solid. 1:50,000. Ordnance Survey for the Geological Survey of Northern Ireland, Southampton.
German, C.R., Higgs, N.C., Thomspon, J., Mills, R., Elderfield, J., Blusztajn, A.P., Fleer, M.P., Bacon, A., 1993. A geochemical study of metalliferous sediment from the TAG hydrothermal mound, 26°08′N, Mid-Atlantic Ridge. J. Geophys. Res. 98, 9683–9692.
Goodfellow, W.D., 2007. Metallogeny of the Bathurst Mining Camp, Northern New Brunswick. In: Goodfellow, W.D. (Ed.), Mineral Deposits of Canada: A Synthesis of Major Deposit Types, District Metallogeny, the Evolution of Geological Provinces, and Exploration Methods. Geological Association of Canada, Mineral Deposits Division, Special Publication 5, pp. 44–469.
Grenne, T., Slack, J.F., 2003. Paleozoic and Mesozoic silica-rich seawater: evidence from hematitic chert (jasper) deposits. Geology 31, 319–332.
Grenne, T., Slack, J.F., 2005. Geochemistry of jasper beds from the Ordovician Løkken Ophiolite, Norway: origin of proximal and distal siliceous exhalites. Econ. Geol. 100, 1511–1527.
Grenne, T., Vokes, F.M., 1990. Sea-floor sulfides at the Hoydal volcanogenic deposit, central Norweigan Caledonides. Econ. Geol. 85, 344–359.
Grenne, T., Ihlen, P.M., Vokes, F.M., 1999. Scandinavian-Caledonide metallogeny in a plate tectonic perspective. Mineral. Deposita 34, 422–471.
Gross, G.A., 1980. A classification of iron formations based on depositional environments. Can. Mineral. 18, 215–222.
Gross, G.A., 1983. Tectonic systems and the deposition of iron-formation. Precambrian Res. 20, 171–187.
Halbach, M., Halbach, P., Lueders, V., 2002. Sulfide-impregnated and pure silica precipitates of hydrothermal origin from the central Indian Ocean. Chem. Geol. 182, 357–375.
Hart, T.R., Gibson, H.L., Lesher, C.M., 2004. Trace element geochemistry and petrogenesis of felsic volcanic rocks associated with volcanogenic massive Cu–Zn–Pb sulfide deposits. Econ. Geol. 99, 1003–1013.
Hartley, J.J., 1933. The geology of north-eastern Tyrone and the adjacent portions of County Londonderry. Proceedings of the Royal Irish Academy, Section B-Biological, Geological and, Chemical Science 41, 218–285.
Hekinian, R., Hoffert, M., Larqué, P., Cheminée, J.L., Stoffers, P., Bideau, D., 1993. Hydrothermal Fe and Si oxyhydroxide deposits from South Pacific intraplate volcanoes and East Pacific Rise axial and off-axial regions. Econ. Geol. 88, 2099–2121.
Herrington, R., Maslennikov, V., Zaykov, V., Seravkin, I., Kosarev, A., Buschmann, B., Orgeval, J.-J., Holland, N., Tesalina, S., Nimis, P., Armstrong, R., 2005. 6: classification of VMS deposits: lessons from the South Uralides. Ore Geol. Rev. 27, 203–237.
Hollis S.P., 2012. Licence DG2. Period—1st January 2010 to 31st December 2011. Technical Report. Submitted to Department of Enterprise, Trade and Investment and Crown Mineral Agent. Unpublished report.
Hollis S.P., 2013. Evolution and mineralization of volcanic arc sequences: Tyrone Igneous Complex, Northern Ireland. Unpublished PhD thesis, University of Southampton, UK.
Hollis, S.P., Roberts, S., Cooper, M.R., Earls, G., Herrington, R.J., Condon, D.J., Cooper, M.J., Archibald, S.M., Piercey, S.J., 2012. Episodic-arc ophiolite emplacement and the growth of continental margins: late accretion in the Northern Irish sector of the Grampian–Taconic orogeny. GSA Bull. 124, 1702–1723.
Hollis, S.P., Cooper, M.R., Roberts, S., Earls, G., Herrington, R.J., Condon, D.J., Daly, J.S., 2013a. Late obduction of the Tyrone ophiolite, Northern Ireland, during the Grampian-Taconic orogeny: a correlative of the Annieopsquotch ophiolite of Newfoundland? J. Geol. Soc. Lond. 170, 861–876.
Hollis, S.P., Cooper, M.R., Roberts, S., Herrington, R.J., Earls, G., Condon, D.J., 2013b. Stratigraphic, geochemical and U–Pb zircon age constraints from Slieve Gallion, Northern Ireland: a correlation of the Irish Caledonian arcs. J. Geol. Soc. Lond. 170, 737–752.
Hollis, S.P., Roberts, S., Earls, G., Herrington, R., Cooper, M.R., Piercey, S.J., Archibald, S.M., Moloney, M., 2014. Petrochemistry and hydrothermal alteration within the Tyrone Igneous Complex, Northern Ireland: implications for VMS mineralization in the peri-Laurentian British and Irish Caledonides. Mineral. Deposita 49, 575–593.
Hollis, S.P., Cooper, M.R., Earls, G., Roberts, S., Herrington, R.J., Piercey, S.J., 2015. Using Tellus data to enhance targeting of volcanogenic massive sulphide mineralisation in the Tyrone Igneous Complex. In: Young, M. (Ed.), Impacts of the Tellus Projects. Royal Irish Academy (in press).
Hutton, D.H.W., 1983. Report on the geology of the central part of prospecting licence 80 N.I. Unpublished report for Ulster Base Metals Limited.
Hutton, D.H.W., Aftalion, M., Halliday, A.N., 1985. An Ordovician ophiolite in County Tyrone, Ireland. Nature 315, 310–312.
Jenner, G.A., 1996. Trace element geochemistry of igneous rocks: Geochemical nomenclature and analytical geochemistry. In: Wyman, D.A. (Ed.), Trace Element Geochemistry of Volcanic Rocks: Applications for Massive Sulfide Exploration. Geological Association of Canada, Short Course Notes 12, pp. 51–77.
Jones, S., Gemmell, B.J., Davidson, G.J., 2006. Petrographic, geochemical, and fluid inclusion evidence for the origin of siliceous cap rocks above volcanic-hosted massive sulfide deposits at Myra Falls, Vancouver Island, British Columbia, Canada. Econ. Geol. 101, 555–584.
Juniper, S.K., Fouquet, Y., 1988. Filamentaous iron-silica deposits from modern and ancient hydrothermal sites. Can. Mineral. 26, 859–869.
Kalogeropoulos, S.I., Scott, S.D., 1983. Mineralogy and geochemistry of tuffaceous exhalites (tetsusekiei) of the Fukazawa mine, Hokuroku District, Japan. In: Ohmoto, H., Skinner, B.J. (Eds.), The Kuroko and Related Volcanogenic Massive Sulfide DepositsEconomic Geology Monograph 5. The Economic Geology Publishing Company, pp. 412–432.
Kalogeropoulos, S.I., Scott, S.D., 1989. Mineralogy and geochemistry of an Archean tuffaceous exhalite: the Main Contact Tuff, Millenbach mine area, Noranda, Quebec. Can. J. Earth Sci. 26, 88–105.
Le Maitre, R.W. (Ed.), 2004. Igneous rocks: A Classification and Glossary of Terms. 2nd Edition. Recommendations of the International Union of Geological Sciences Subcommission on the Systematics of Igneous Rocks. Cambridge University Press (326 pp.).
Leistel, J.M., Marcoux, E., Deschamps, Y., 1998. Chert in the Iberian Pyrite Belt. Mineral. Deposita 33, 59–81.
Lesher, C.M., Goodwin, A.M., Campbell, I.H., Gorton, M.P., 1986. Trace-element geochemistry of ore-associated and barren, felsic metavolcanic rocks in the Superior province, Canada. Can. J. Earth Sci. 23, 22–237.
Leyshon, P.R., Cazalet, P.C.D., 1978. Base-metal exploration programme in Lower Palaeozoic volcanic rocks, Co. Tyrone, Northern Ireland. Bull. Inst. Min. Metall. 85, B91–B99.
Liaghat, S., MacLean, W.H., 1992. The Key Tuffite, Matagami mining district: origin of the tuff component and mass changes. Explor. Min. Geol. 1, 197–207.
Maslennikov, V.V., Ayupova, N.R., Herrington, R.J., Danyushevskiy, L.V., Large, R.R., 2012. Ferruginous and manganiferous haloes around massive sulphide deposits of the Urals. Ore Geol. Rev. 47, 5–41.
McConnell, B.J., Stillman, C.J., Hertogen, J., 1991. An Ordovician basalt to peralkaline rhyolite fractionation series from Avoca, Ireland. J. Geol. Soc. Lond. 148, 711–718.
McDonough, W.F., Sun, S.-S., 1995. The composition of the earth. Chem. Geol. 120, 223–254.
Michard, A., Albarède, F., 1986. The REE content of some hydrothermal fluids. Chem. Geol. 55, 51–60.
Miller, C., Halley, S., Green, G., Jones, M., 2001. Discovery of the West 45 volcanic-hosted massive sulfide deposit using oxygen isotopes and REE geochemistry. Econ. Geol. 96, 1227–1237.
Mills, R.A., Elderfield, H., 1995. Rare earth element geochemistry of hydrothermal deposits from the active TAG mound, 26°N Mid-Atlantic Ridge. Geochim. Cosmochim. Acta 59, 3511–3524.
Mitra, A., Elderfield, H., Greaves, M.J., 1994. Rare earth elements in submarine hydrothermal fluids and plumes from the Mid-Atlantic Ridge. Mar. Chem. 46, 217–235.
Peatfield, G.R., 2003. Updated technical review report on the Tyrone mineral exploration property, prospecting licences UM 11/96 and UM 12/96, County Tyrone, Northern Ireland — 20 January, 2003. Report for Tournigan Gold Corporation.
Peter, J.M., 2003. Ancient iron-rich metalliferous sediments (iron formations): their genesis and use in the exploration for stratiform base metal sulphide deposits, with examples from the Bathurst Mining Camp. In: Lentz, D.R. (Ed.),

Geochemistry of Sediments and Sedimentary Rocks: Evolutionary Considerations to Mineral Deposit Forming Environments. GEOtext 4. Geological Association of Canada, pp. 145–173.
Peter, J.M., Goodfellow, W.D., 1996. Mineralogy, bulk and rare earth element geochemistry of massive sulphide-associated hydrothermal sediments of the Brunswick Horizon, Bathurst Mining Camp, New Brunswick. Can. J. Earth Sci. 33, 252–283.
Peter, J.M., Goodfellow, W.D., 2003. Hydrothermal sedimentary rocks of the Heath Steele Belt, Bathurst Mining Camp, New Brunswick. Part 3. Application of mineralogy and mineral and bulk compositions to massive sulfide exploration. Econ. Geol. Monogr. 11, 317–433.
Piercey, S.J., 2007. Volcanogenic massive sulphide (VMS) deposits of the Newfoundland Appalachians: an overview of their setting, classification, grade-tonnage data, and unresolved questions. In: Pereira, C.G.P., Walsh, D.G. (Eds.), Current Research. Newfoundland Department of Natural Resources, Geological Survey, Report 07-01, pp. 169–178.
Piercey, S.J., Hinchey, J., 2012. Field Trip Guide Book — B4. Volcanogenic massive sulphide (VMS) deposits of the Central Mobile Belt, Newfoundland. GAC-MAC-AGC-AMC Joint Annual Meeting, St. John's, Canada.
Piper, D.Z., 1974. Rare earth elements in the sedimentary cycle: a summary. Chem. Geol. 14, 285–304.
Pollock, J.C., Hibbard, J.P., Sylvester, P.J., 2009. Early Ordovician rifting of Avalonia and birth of the Rheic Ocean: U–Pb detrital zircon constraints from Newfoundland. J. Geol. Soc. Lond. 166, 501–515.
Slack, J.F., 2012. Exhalites. In: Shanks III, W.C., Thurston, R. (Eds.), Volcanogenic Massive Sulfide Occurrence Model. Scientific Investigations Report 2010-5070-C, pp. 157–163.
Slack, J.F., Foose, M.P., Flohr, M.J.K., Scully, M.V., Belkin, H.E., 2003. Exhalative and subseafloor replacement processes in the formation of the Bald Mountain massive sulfide deposit, northern Maine. Econ. Geol. Monogr. 11, 513–547.
Slack, J.F., Grenne, T., Bekker, A., Rouxel, O.J., Lindberg, P.A., 2007. Suboxic deep seawater in the late Paleoproterozoic: evidene from hematitic chert and iron formation related to seafloor-hydrothermal sulfide deposits, central Arizona, USA. Earth Planet. Sci. Lett. 225, 243–256.
Slack, J.F., Grenne, T., Bekker, A., 2009. Seafloor-hydrothermal Si–Fe–Mn exhalites in the Pecos greenstone belt, New Mexico, and the redox state of ca. 1720 Ma deep seawater. Geosphere 5, 302–314.
Spry, P.G., Peter, J.M., Slack, J.F., 2000. Meta-exhalites as exploration guides to ore. In: Spry, P.G., Marshall, B., Vokes, F.M. (Eds.), Metamorphosed and Metamorphic Ore Deposits. Reviews in Economic Geolog 11, pp. 163–201.
Stow, D., 2005. Sedimentary Rocks in the Field. A Colour Guide. Manson Publishing (320 pp.).
Sverjensky, D.A., 1984. Europium redox equilibria in aqueous solution. Earth Planet. Sci. Lett. 67, 70–78.
Thurlow, J.G., 2010. Great Mining Camps of Canada 3. The history and geology of the Buchans mine, Newfoundland and Labrador. Geosci. Can. 37, 145–173.
Toyoda, J., Masuda, A., 1991. Chemical leaching of pelagic sediments: identification of the carrier of the Ce anomaly. Geochem. J. 25, 95–119.
Tsutsumi, M., Ohmoto, H., 1983. A preliminary oxygen isotope study of Tetsusekiei ores associated with the Kuroko Deposits in the Hokuroku District, Japan. In: Ohmoto, H., Skinner, B.J. (Eds.), The Kuroko and Related Volcanogenic Massive Sulfide DepositsEconomic Geology Monograph 5. The Economic Geology Publishing Company, pp. 433–438.
van Staal, C.R., 2007. Pre-Carboniferous tectonic evolution and metallogeny of the Canadian Appalachians. In: Goodfellow, W.D. (Ed.), Mineral deposits of Canada: a synthesis of major deposit types, district metallogeny, the evolution of geological provinces, and exploration methods. Geological Association of Canada, Mineral Deposits Division, Special Publication 5, pp. 793–818.
van Staal, C.R., Whalen, J.B., McNicoll, V.J., Pehrsson, S.J., Lissenberg, C.J., Zagorevski, A., Van Breeman, O., Jenner, G.A., 2007. The Notre Dame arc and the Taconic Orogeny in Newfoundland. In: Hatcher, J., Carlson, M.P., McBride, J.H., Martínez Catalán, J.R. (Eds.), The 4D Framework of Continental Crust. Geological Society of America, Memoirs 200, pp. 511–552.
Young, M.E., Donald, A.W., 2013. A guide to the Tellus data. Geological Survey of Northern Ireland, Belfast, p. 233.
Zagorevski, A., 2008. Preliminary geochemical database of the Buchans–Robert's Arm Belt, central Newfoundland. Geological Survey of Canada Open File 5986.
Zagorevski, A., vaan Staal, C.R., 2011. The record of Ordovician arc–arc and arc–continent collisions in the Canadian Appalachians during the closure of Iapetus. In: Brown, D., Ryan, P.D. (Eds.), ArcContinent Collision. Frontiers in Earth Sciences, pp. 341–371.
Zagorevski, A., Rogers, N., van Staal, C.R., McNicoll, V., Lissenberg, C.J., Valverde-Vaquero, P., 2006. Lower to Middle Ordovician evolution of peri-Laurentian arc and back-arc complexes in Iapetus: constraints from the Annieopsquotch Accretionary Tract, central Newfoundland. GSA Bull. 118, 324–342.
Zagorevski, A., van Staal, C.R., McNicoll, V.J., Rogers, N., Valverde-Vaquero, P., 2008. Tectonic architecture of an arc–arc collision zone, Newfoundland Appalachians. In: Draut, A.E., Clift, P.D., Scholl, D.W. (Eds.), Formation and Application of the Sedimentary Record in Arc Collision Zones. Geological Society of America, Special Paper, 436, pp. 309–333.
Zagorevski, A., McNicoll, V., van Staal, C.R., Kerr, A., Joyce, N., 2014. From large zones to small terranes to detailed reconstruction of an Early to Middle Ordovician arc–backarc system preserved along the Iapetus Suture Zone: a legacy of Hank Williams. Geosci. Can. 41. http://dx.doi.org/10.12789/geocanj.2014.41.054.